CRYOEM 001 :
TOOLS OF THE TRADE - MICROSCOPES AND DETECTORS

NCCAT Embedded Training — Master Class series

September 30 - October 5, 2020

NATIONAL CENTER FOR
CRYOEM ACCESS & TRAINING

New York Structural
Biology Center

SIMONS ELECTRON
MICROSCOPY CENTER

CRYOEM 001 : SINGLE PARTICLE MASTERCLASS

Introduction to cryoEM: SPA

Building a cryoEM toolkit

EM compatible samples

EM support films and grids

Sample preparation

Tools of the trade:

- microscopes and detectors

Microscope operations

Data collection strategies

Data assessment & QC

Data processing:

- cryoEM IT infrastructure
- On-the-fly feedback
- 3D Reconstruction

Visualization and validation

CRYOEM: SCALE WITHIN BIOLOGY

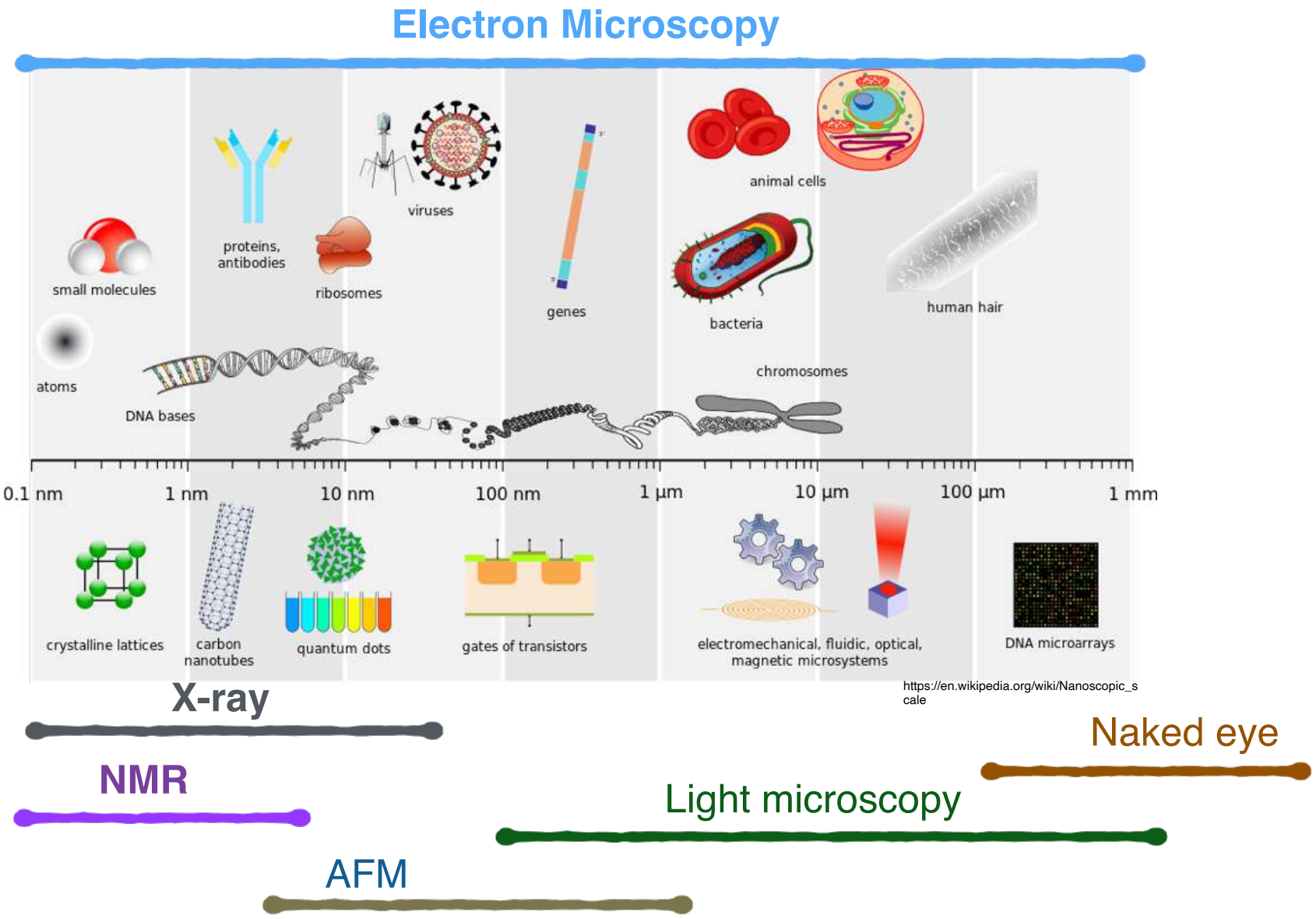

https://en.wikipedia.org/wiki/Nanoscopic_scale

WHAT BROUGHT ABOUT THE RESOLUTION REVOLUTION

(~2012-2014)

Hardware

Microscopes

Direct Detectors

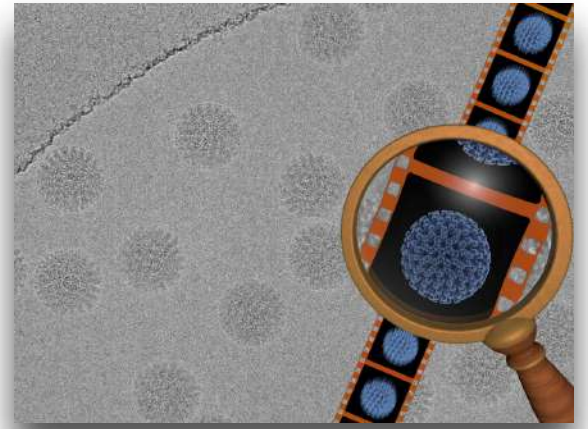

Computers

2012->2017
Cost reduced by 100x

THE ELECTRON MICROSCOPE

Ruska and Knoll in Berlin in the early 1930s

-Wikipedia

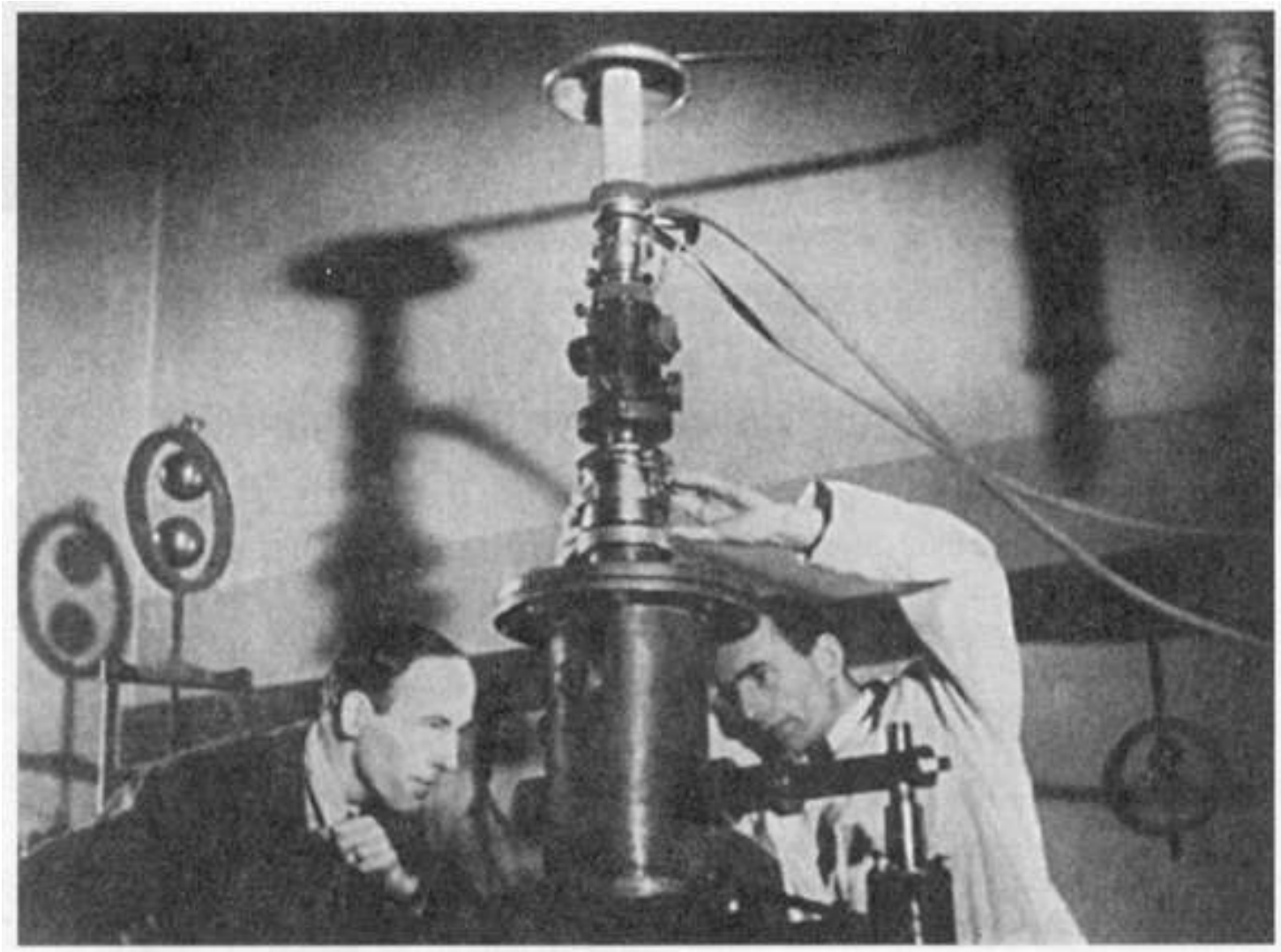

WHY ELECTRONS

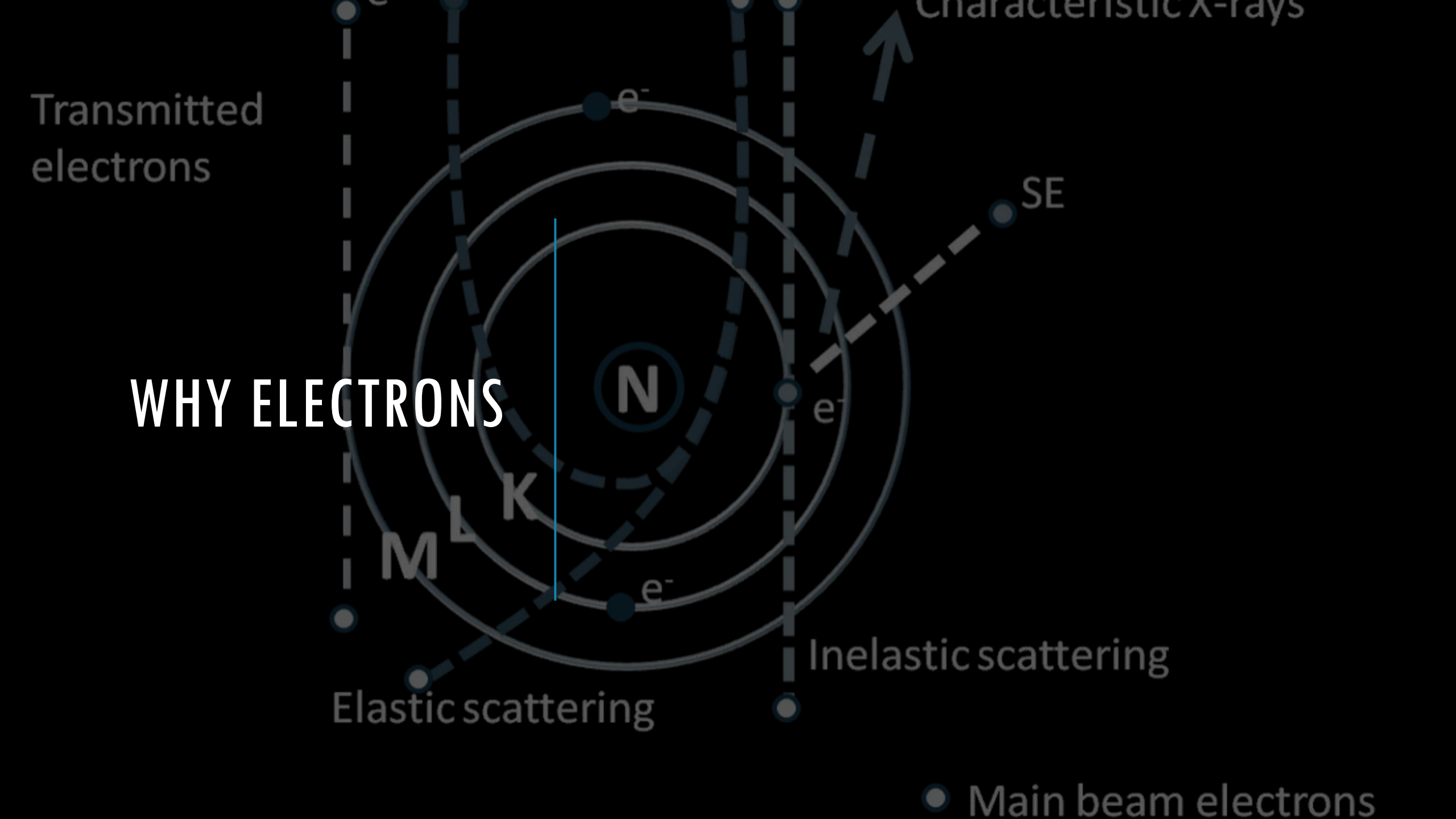

WHY ELECTRONS

Pros	Cons
Small wavelength	Damages sample worse with faster electrons
Can be focused	Poor penetration better with faster electrons

CRYOEM MODALITIES AND TOOLS

Cryo-EM

	Tomography	Single-particle reconstruction	2D Electron crystallography	MicroED
Approach	Imaging	Imaging	Imaging/diffraction	Imaging/diffraction
Sample	Cells or organelles	Single particles	2D crystals	3D crystals
Top resolution		2.2 Å	1.9 Å	1.4 Å
Example	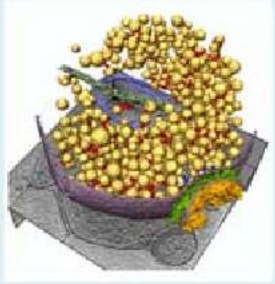			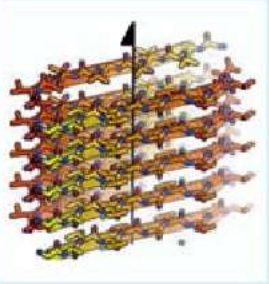

https://doi.org/10.1002/pro.2989

~3.4Å | ~1.2Å | ~1.9Å | ~0.7Å

CRYOEM TOOLS

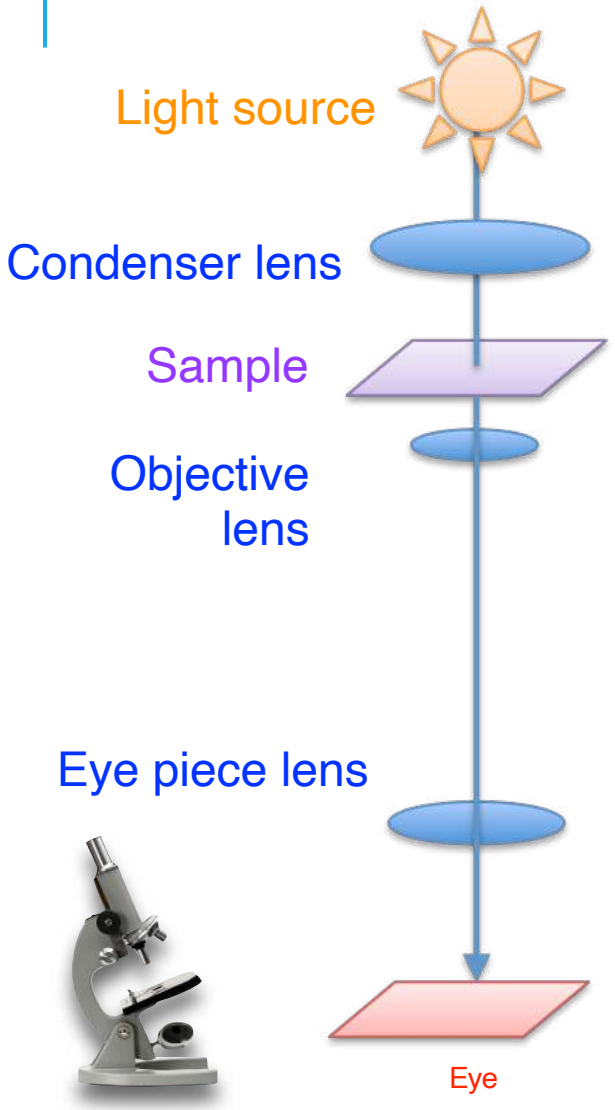

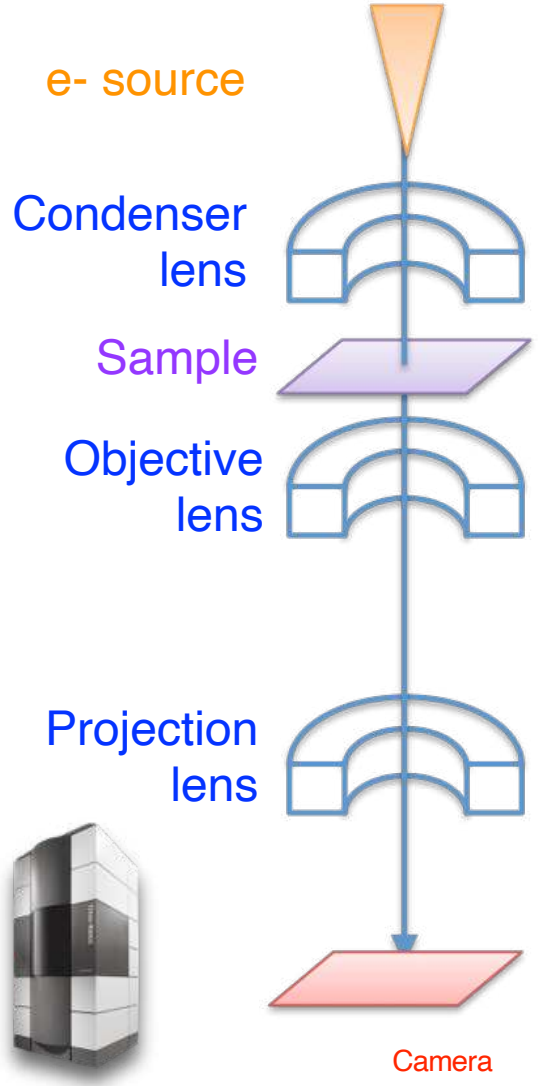

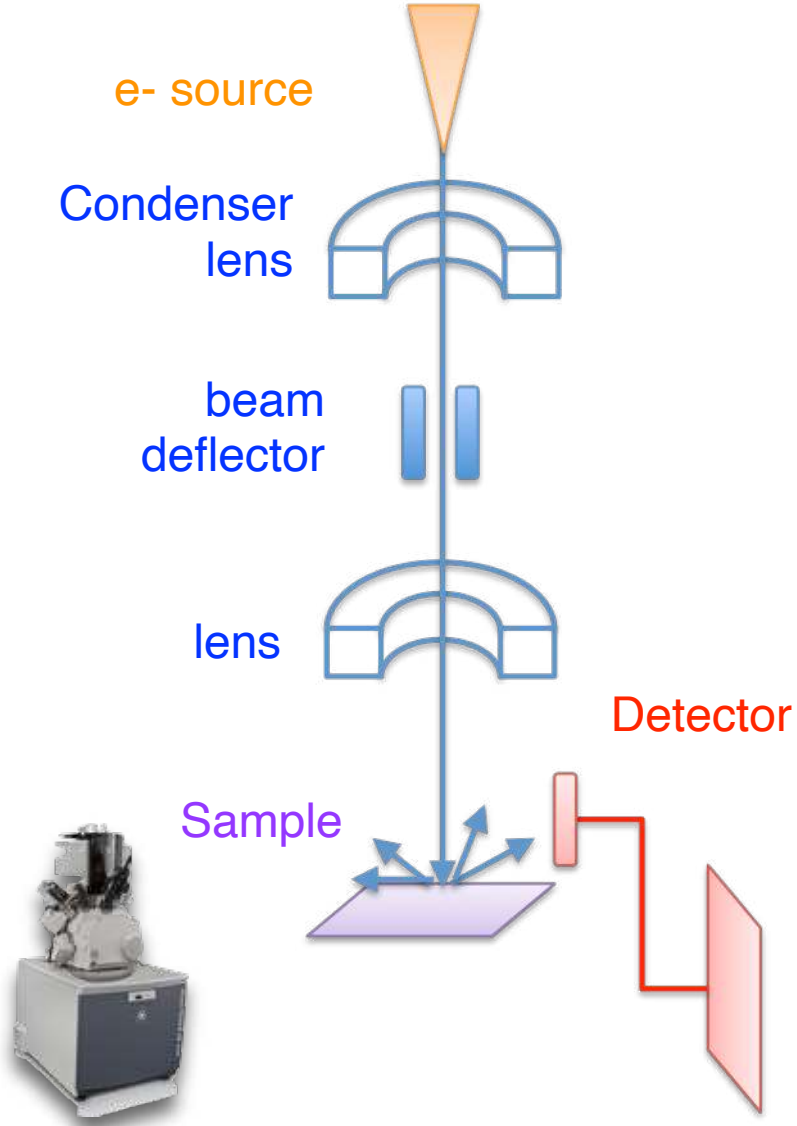

MAIN PARTS OF AN EM

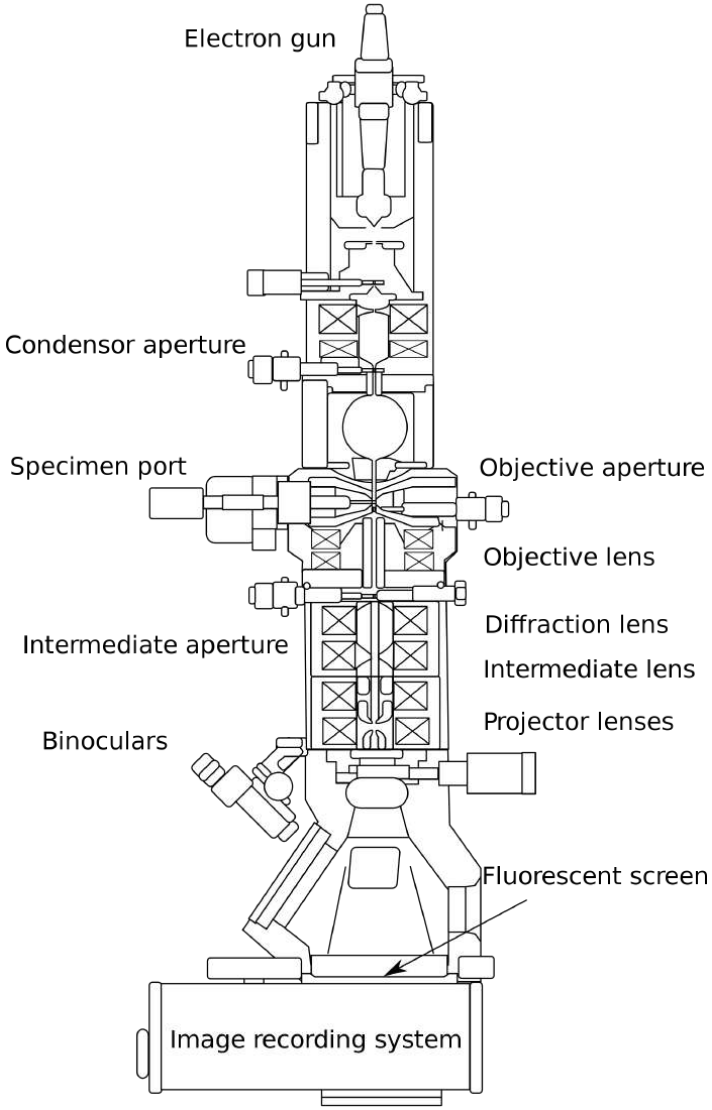

Electron sources

Vacuum systems

Lenses

Detectors

ELECTRON SOURCES

What are the 3 main kinds of electron sources?

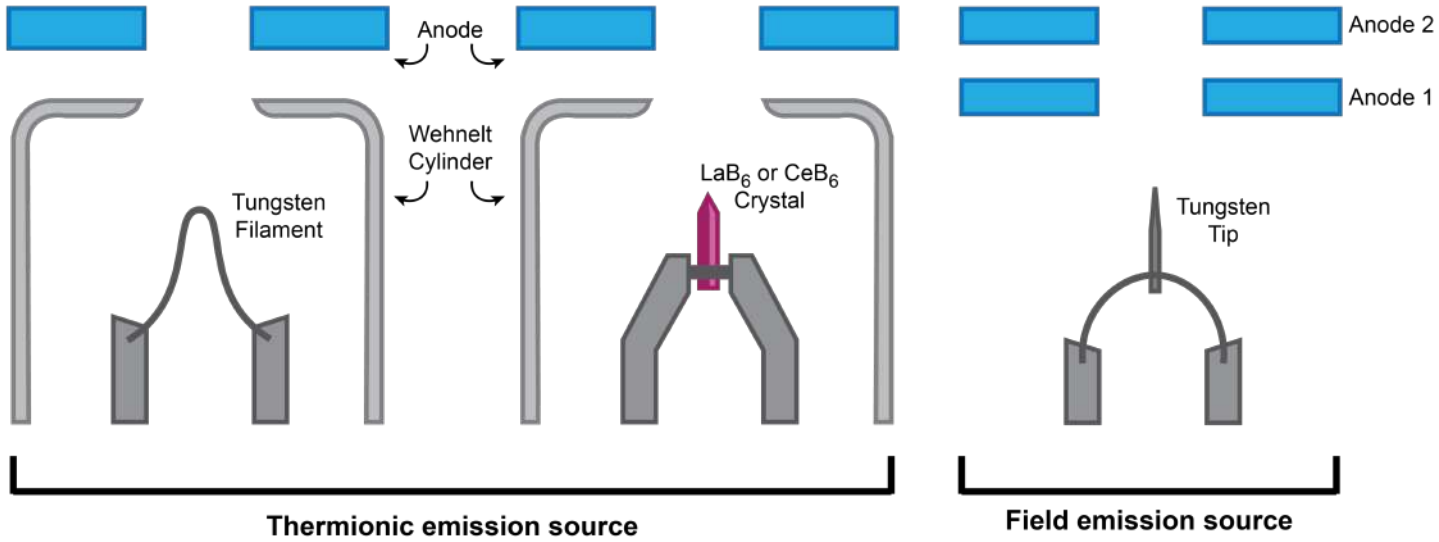

www.thermofisher.com

nanoscience.com

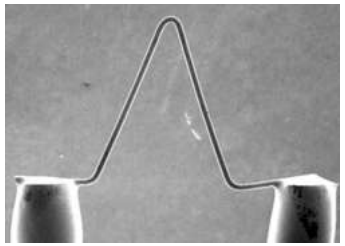

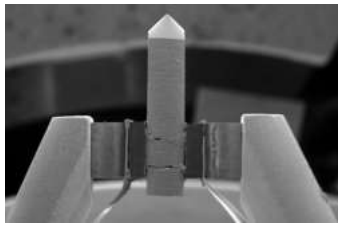

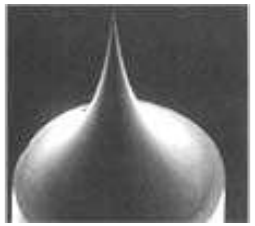

ELECTRON SOURCES

How fast are the electrons moving?

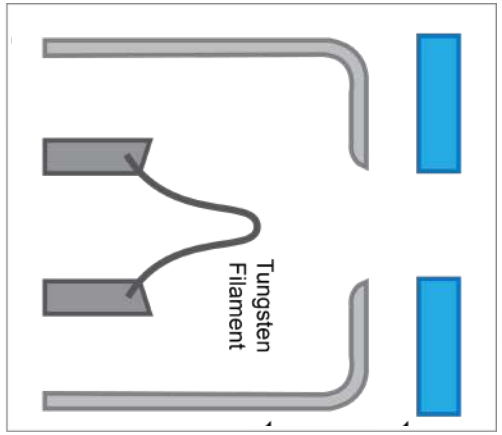

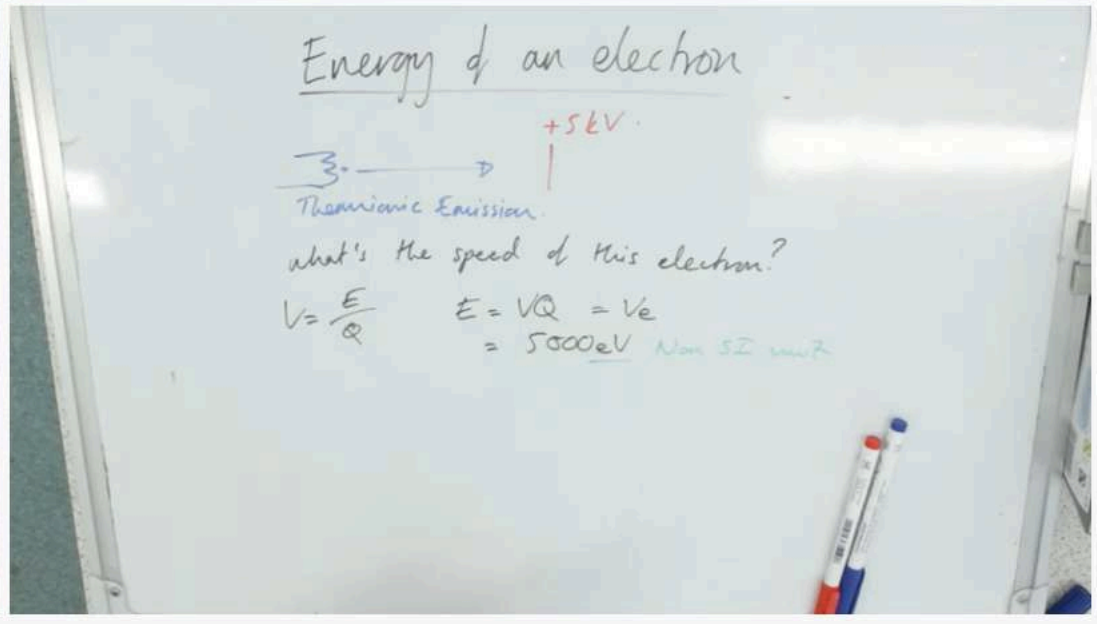

https://www.youtube.com/watch?v=tYCET6vYdYk

ELECTRON SOURCES

How fast are the electrons moving?

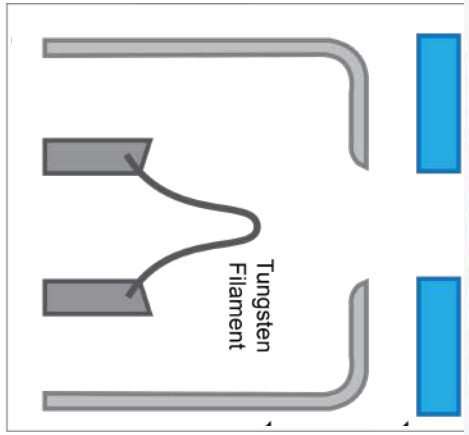

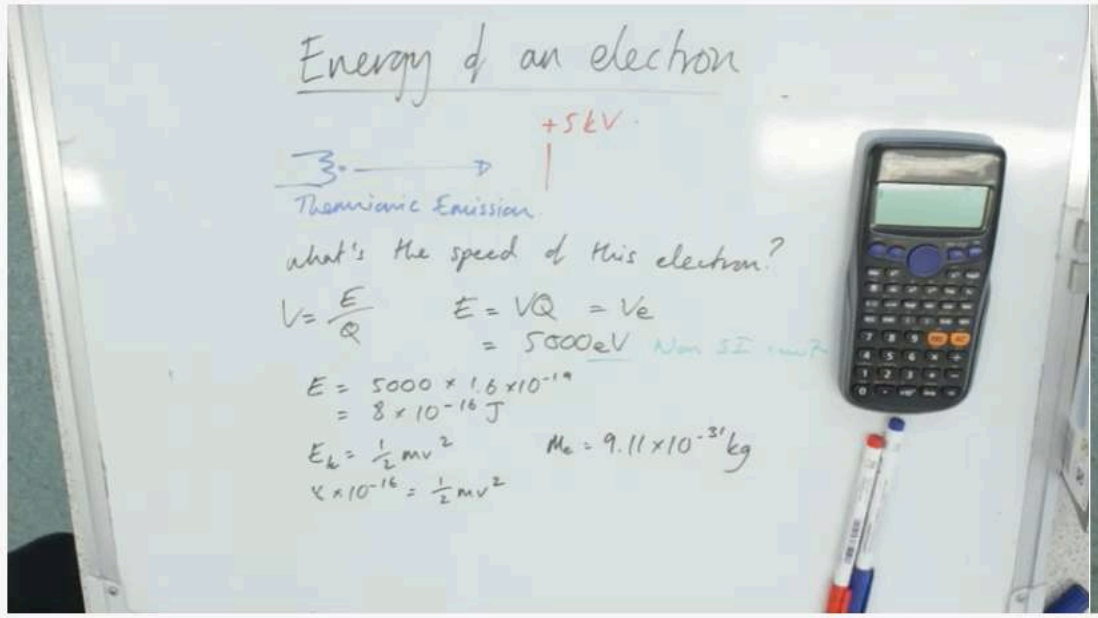

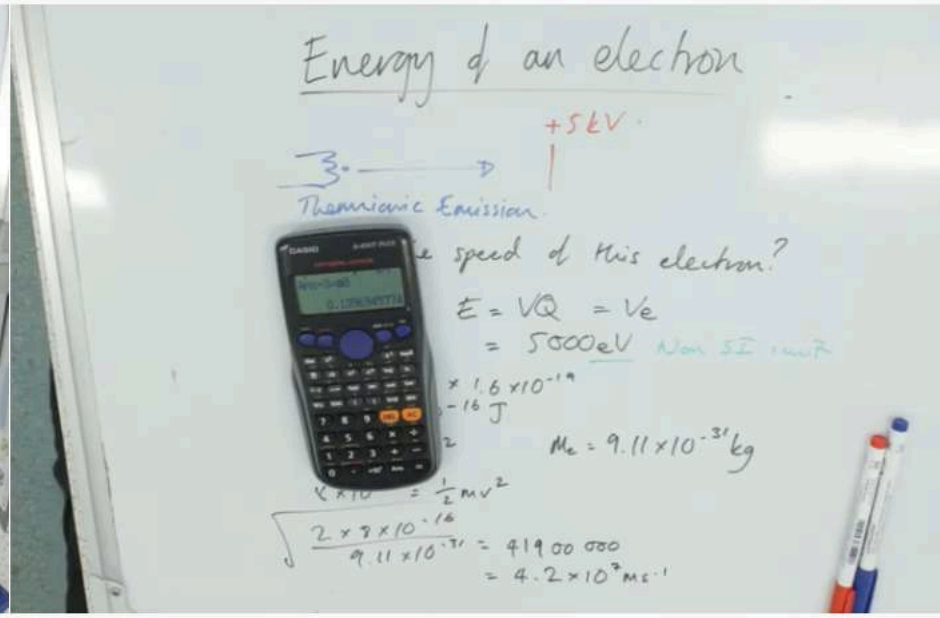

https://www.youtube.com/watch?v=tYCET6vYdYk

ELECTRON SOURCES & TYPES OF EMS

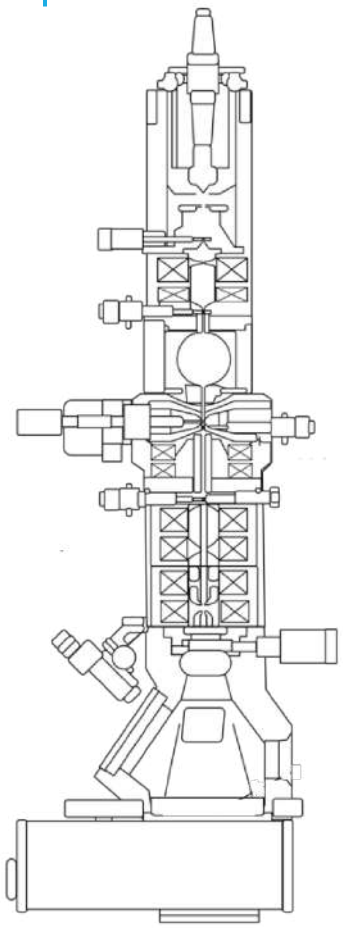

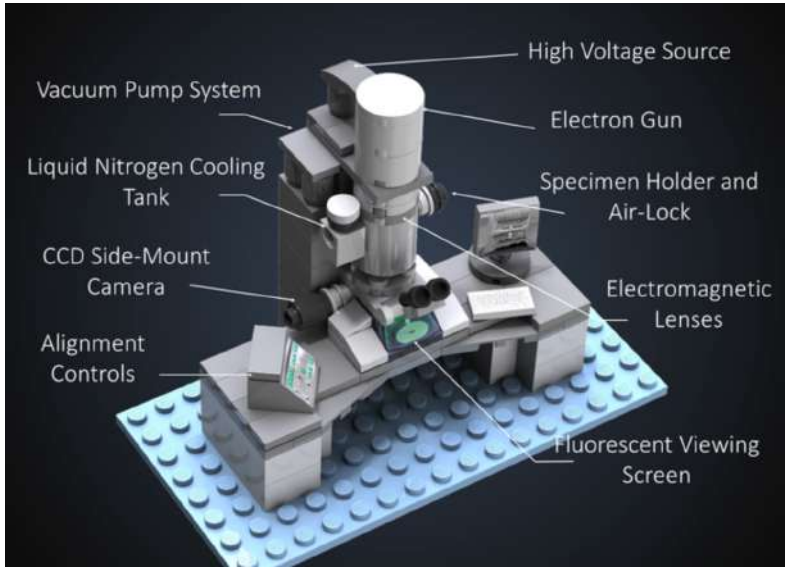

https://ideas.lego.com/projects/102281

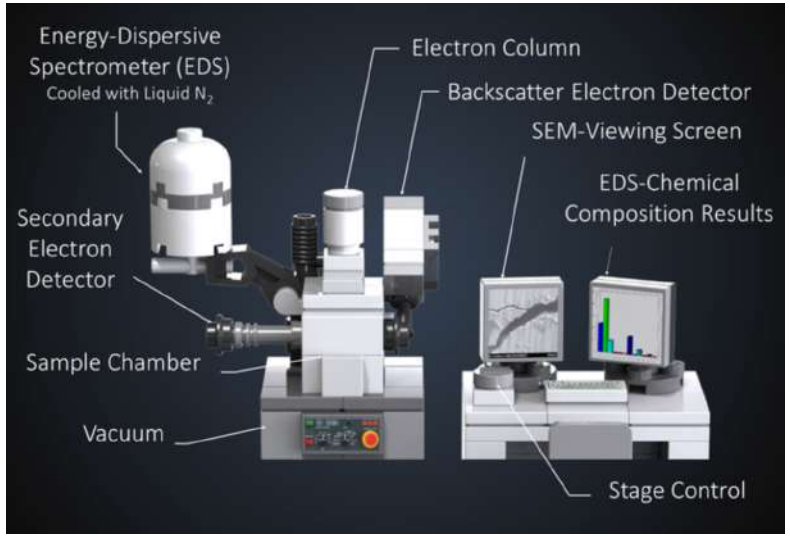

ELECTRON SOURCES & TYPES OF EMS

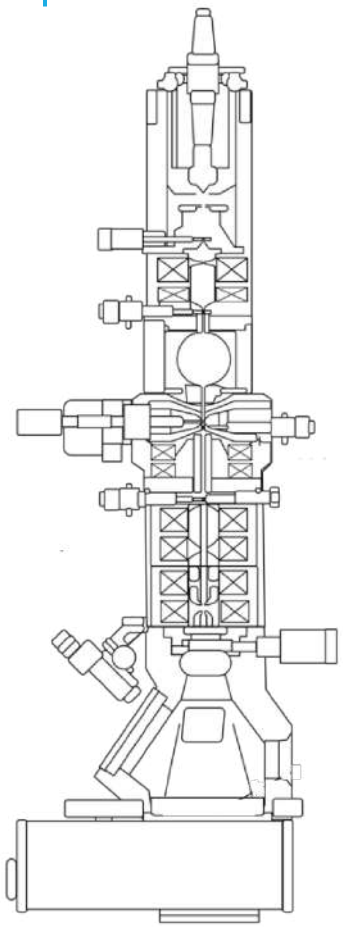

80-120 kV: JEM 1230; Tecnai T12
W or LaB6
High contrast & robust
sub-nm resolution

200 kV: JEM 2100F, Tecnai F20, Talos, Artica
FEG
2+ Å resolution (3.5-4 Å)

300 kV: JEM 3200FSC, cryo-ARM, Krios, Polara
FEG
Smaller effect on unwanted lens aberration
1.5-3 Å resolution

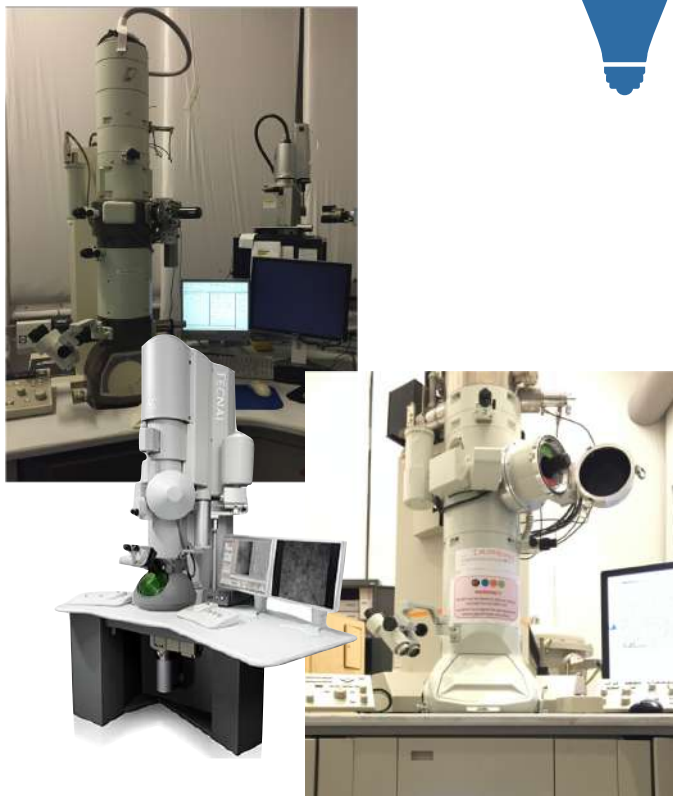

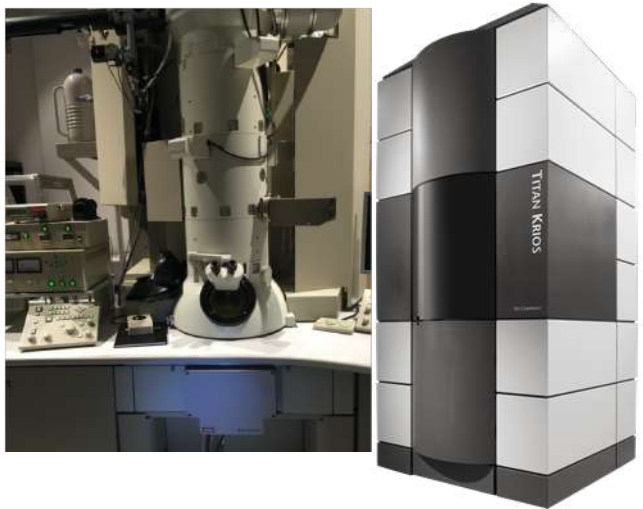

ELECTRON SOURCES & TYPES OF EMS

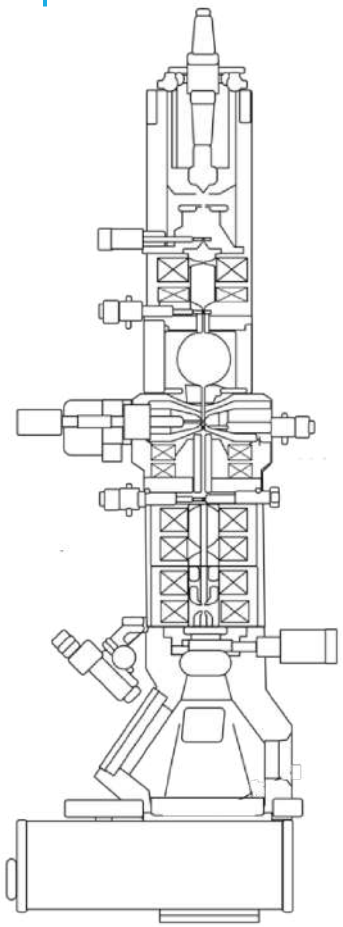

1-1.2 MV: Hitachi, JEOL
LaB6

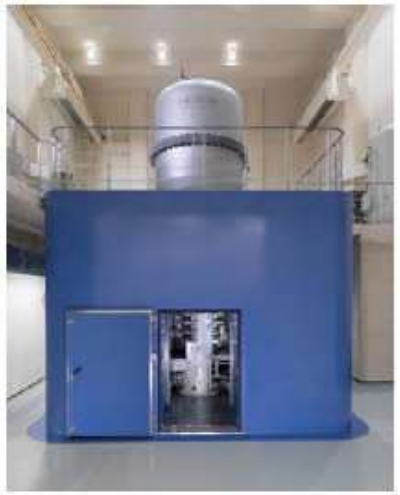

uhvem.osaka-u.ac.jp

3 MV: Hitachi H3000
LaB6

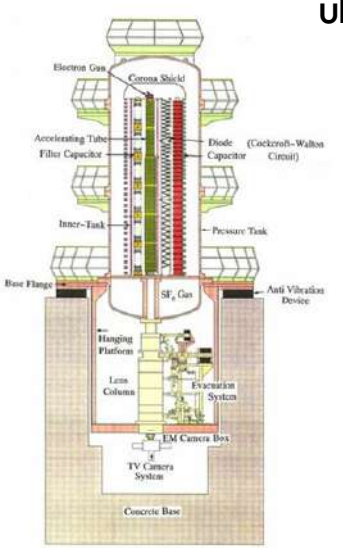

VACUUM SYSTEMS

Why do we need a vacuum?

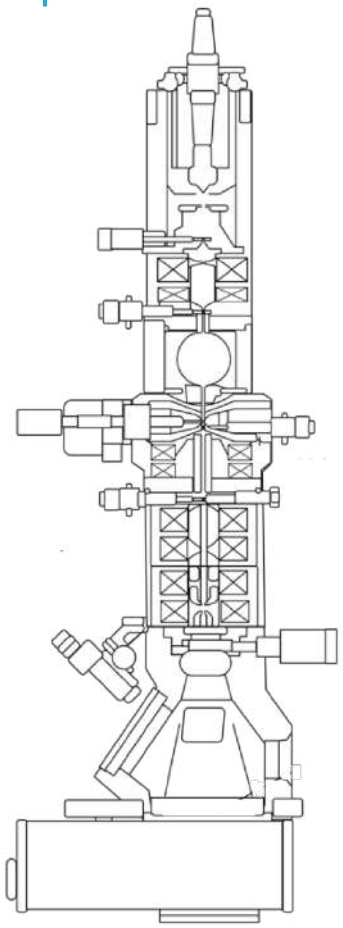

Beam coherence - at STP mean free path ~1 cm

Insulation - interaction between e- and air

Filament - O2 will burn out source

Contamination - reduce interaction gas, e-beam and sample

VACUUM SYSTEMS

What types of pumps do we have?

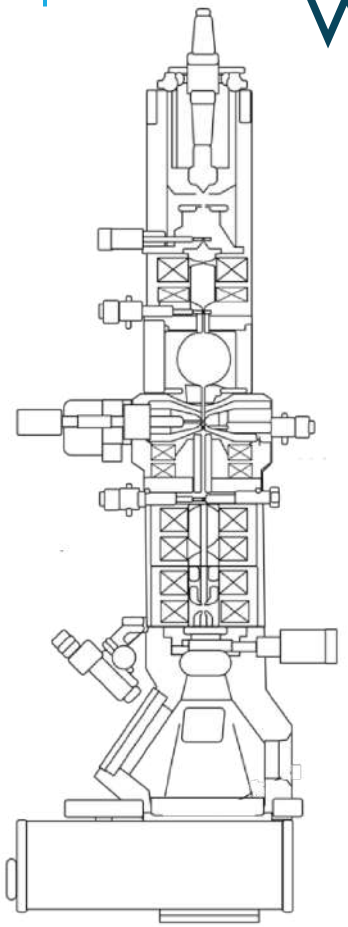

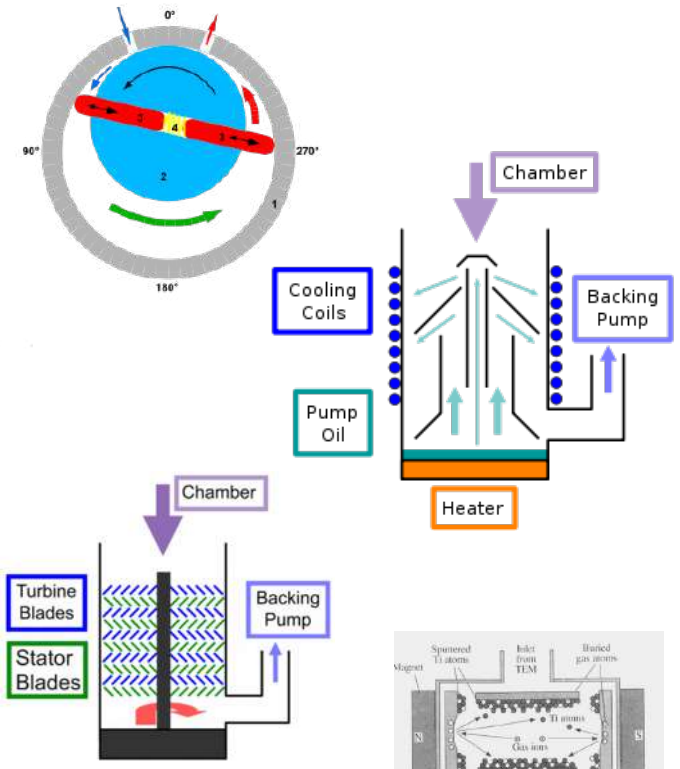

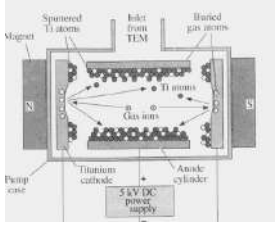

wikipedia.com

1 mm Hg = 1 Torr = 10^2 Pa

1 atm = 760 Torr = 7.5×10^4 Pa

PVP / Rotary $1\text{-}10^{-3}$ Torr | >0.1 Pa

Diffusion $10^{-3}\text{-}10^{-6}$ Torr | $0.1\text{-}10^{-4}$ Pa

Turbo $10^{-6}\text{-}10^{-9}$ Torr | $10^{-4}\text{–}10^{-7}$ Pa

IGP $10^{-9}\text{-}10^{-12}$ Torr | $10^{-7}\text{-}10^{-9}$ Pa

VACUUM SYSTEMS

What types of pumps do we have?

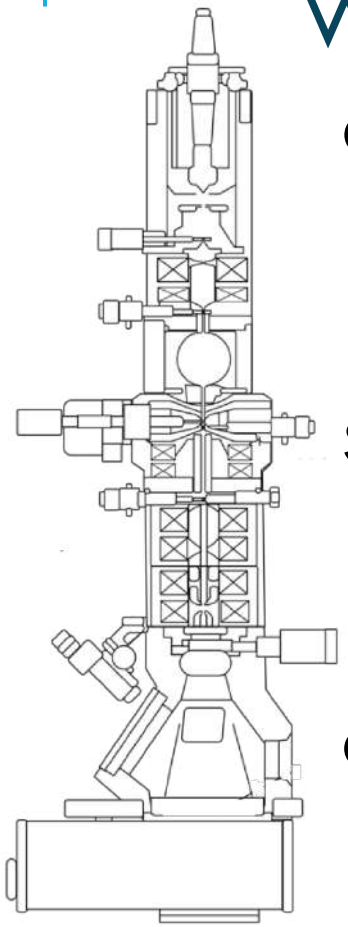

Gun	10^{-9} Torr
Specimen	10^{-6} -10^{-7} Torr
Chamber and Camera	10^{-5} -10^{-6} Torr

1 mm Hg = 1 Torr = 10^2 Pa

1 atm = 760 Torr = 7.5×10^4 Pa

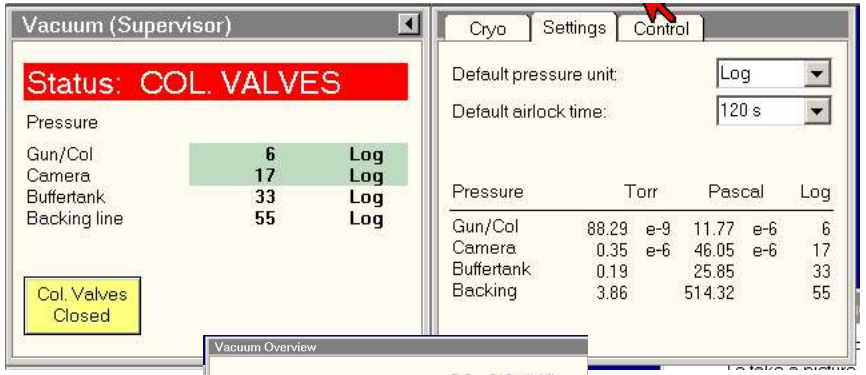

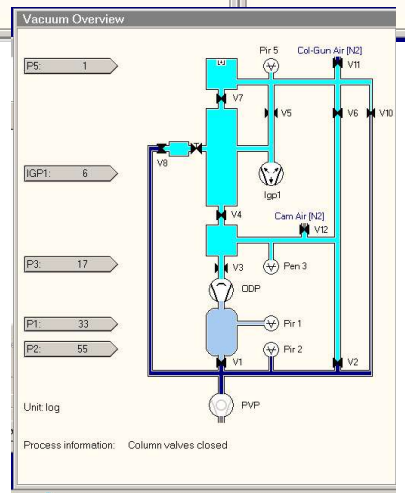

VACUUM SYSTEMS

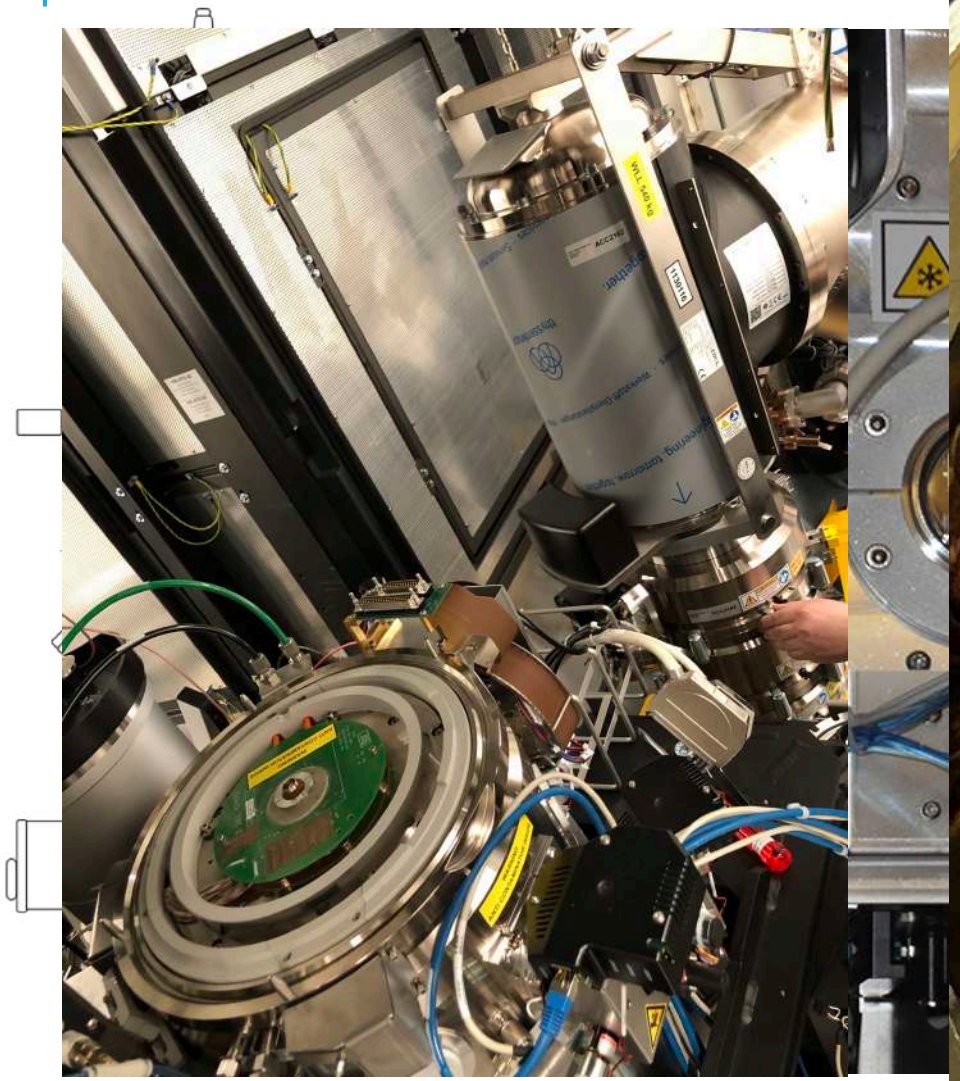

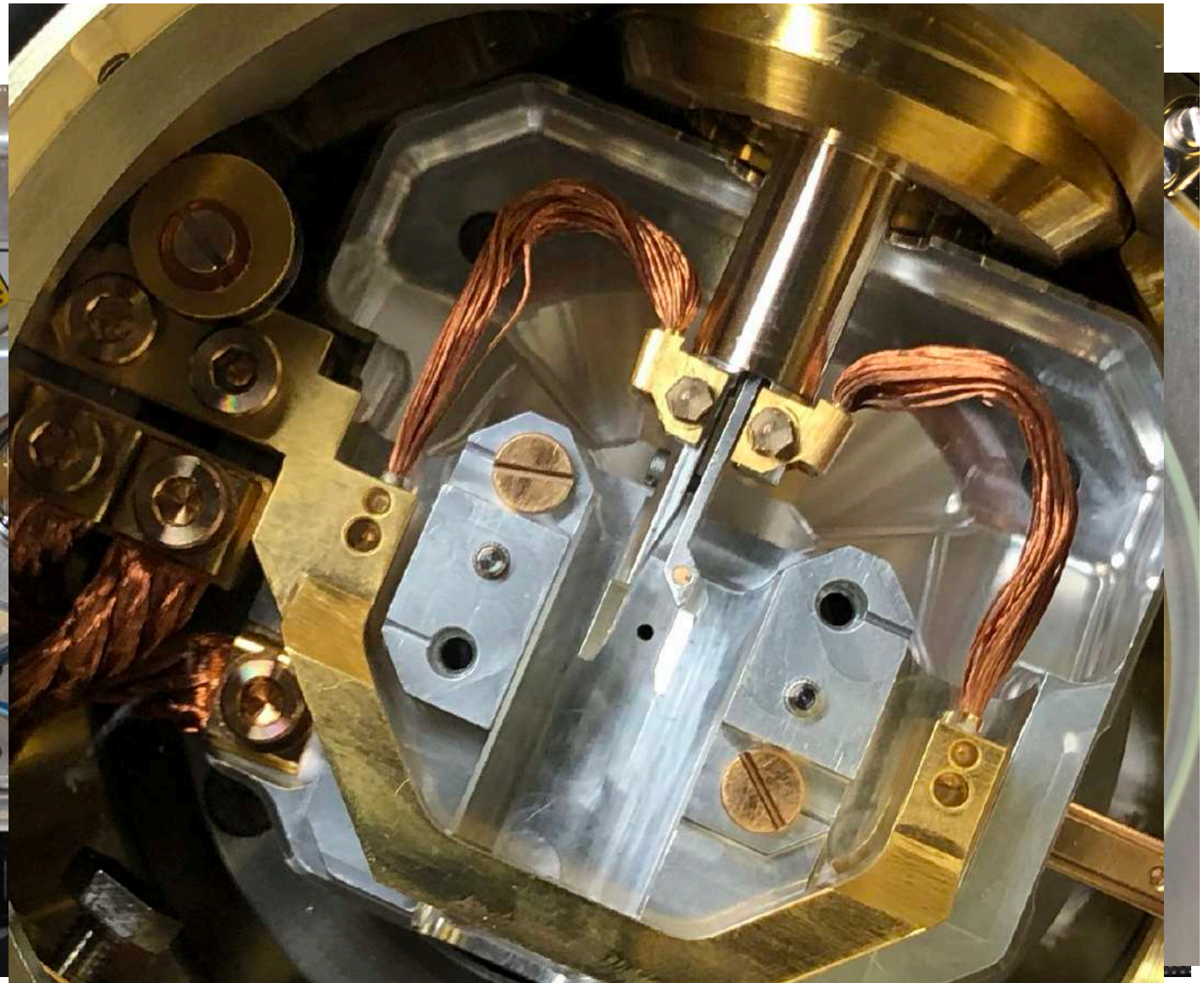

LENSES

What types of lenses do we have?

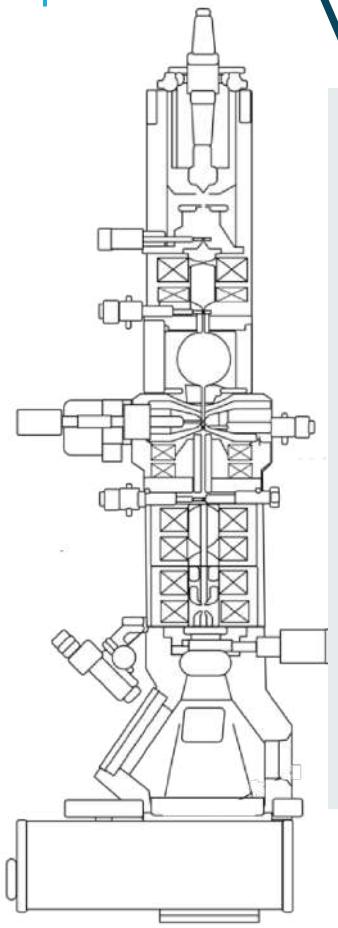

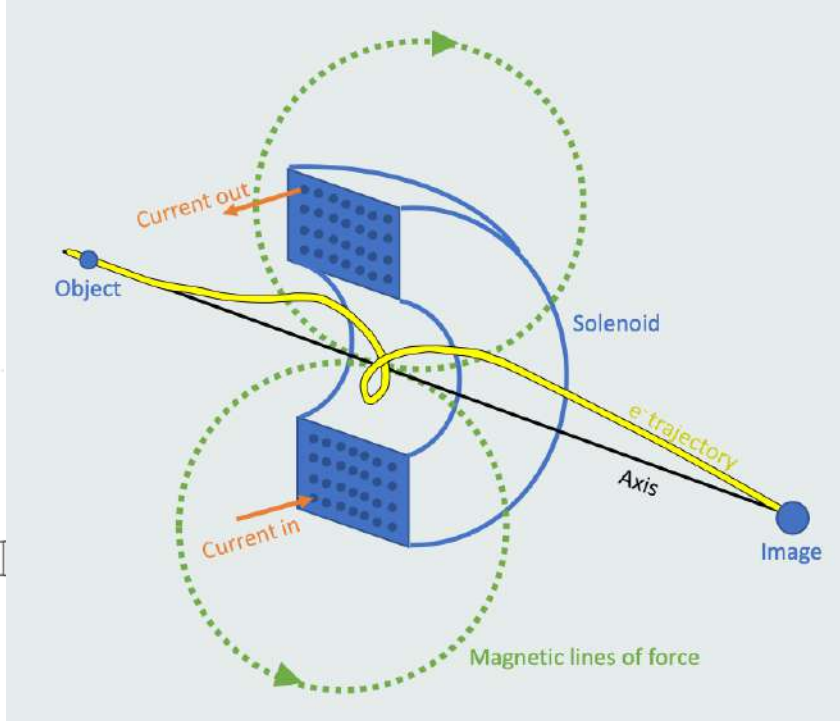

- Focus
- Magnify
- Rotate

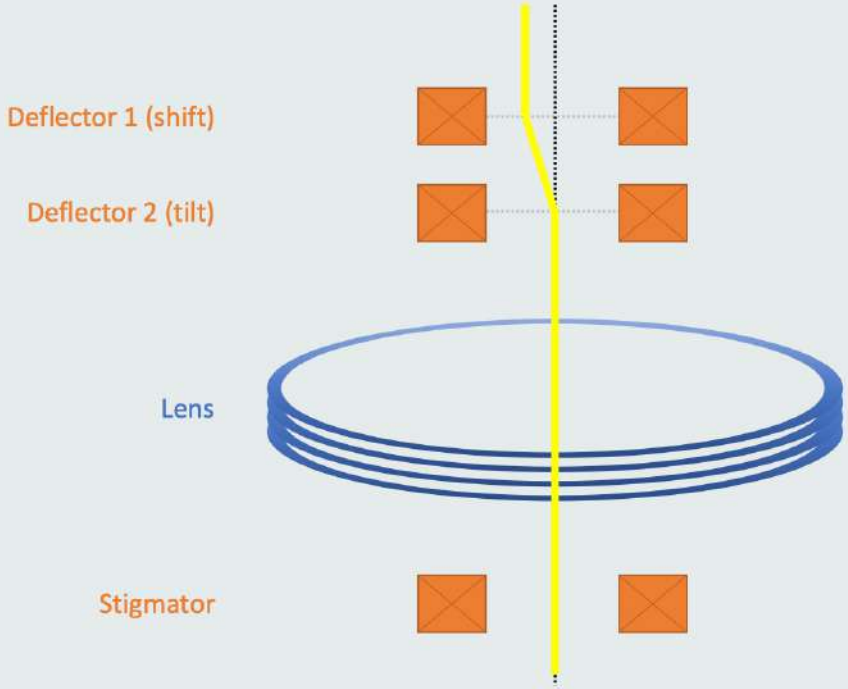

LENSES

Microscope Alignments
What to do & what not to do

Do:

- Start at eucentric height and focus
- Check if it is already good before attempt
- Align from top to bottom

Not to do:

- ~~Align without a way to undo~~
- ~~Align when TEM is not stable~~ (i.e., ~~temperature)~~

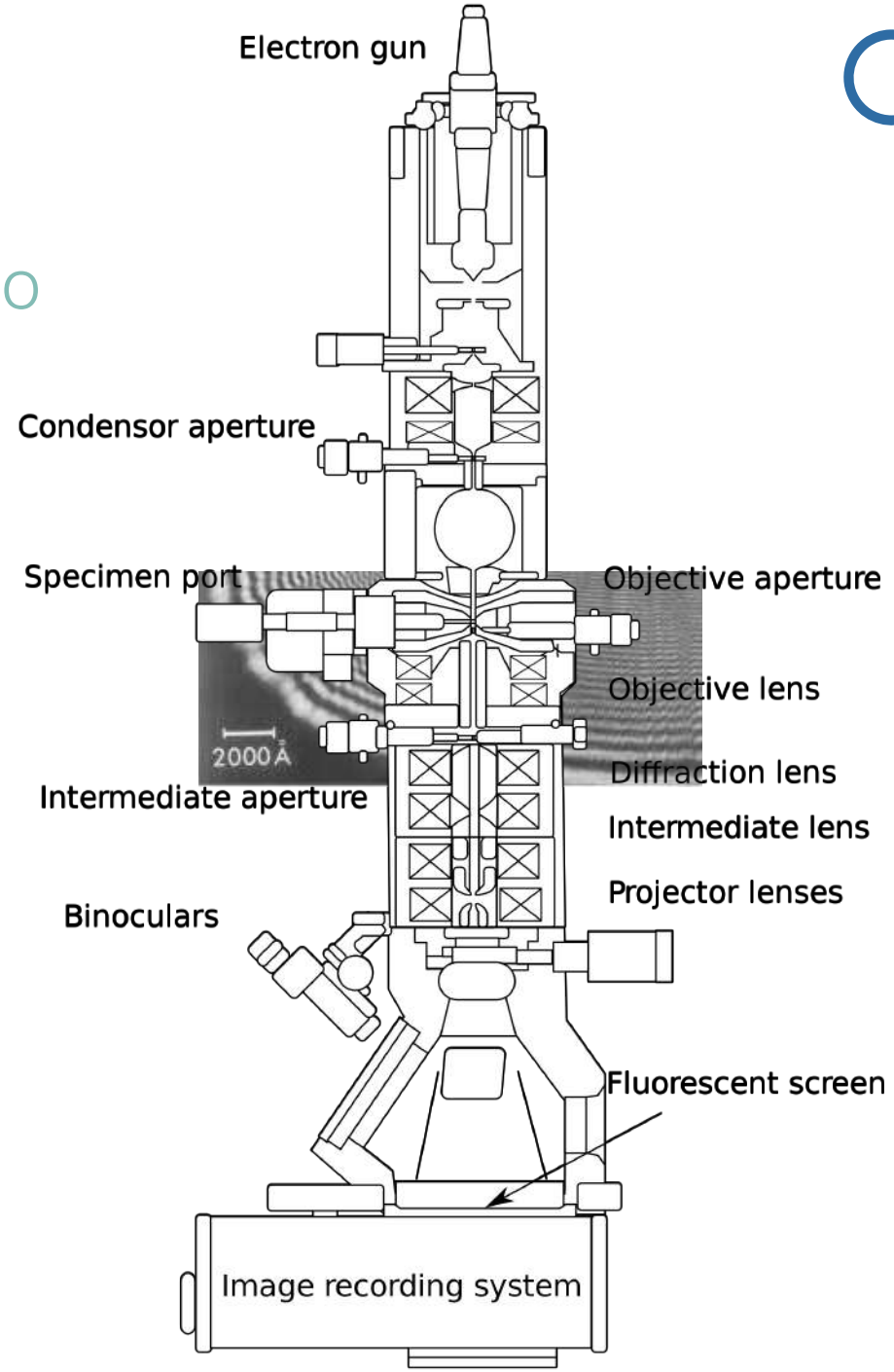

DETECTORS

Digital Cameras for TEM

Photon converted

Direct sensing

?

- CCD — Charge Coupled Device
- CMOS — Complementary Metal Oxide Semiconductor

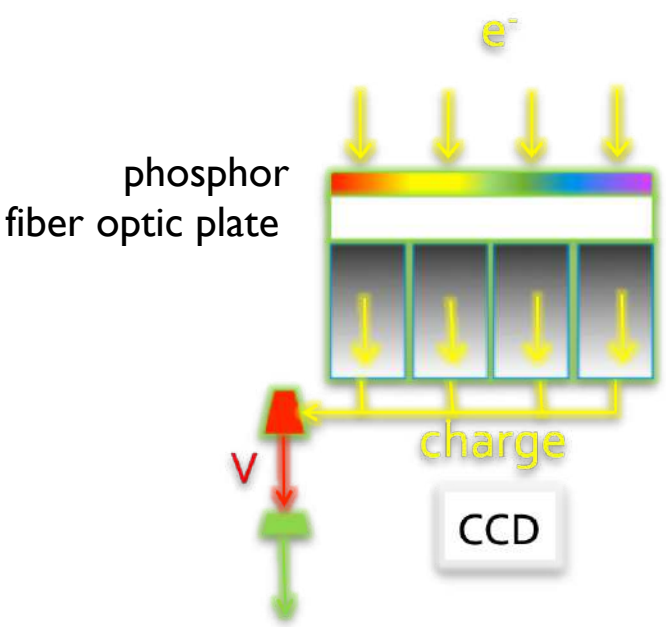

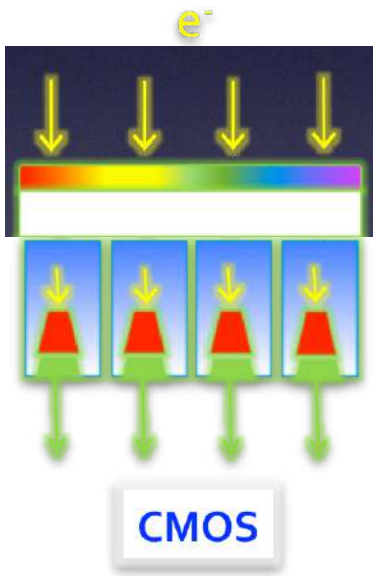

high dose rate

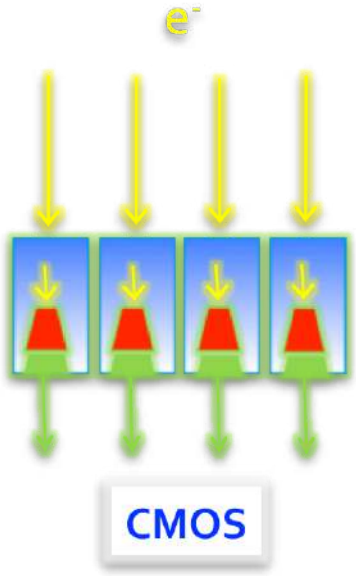

Direct Detectors

DETECTORS

Detector Performance Characterization

MTF (Modulation Transfer Transform)
contribute to signal envelope

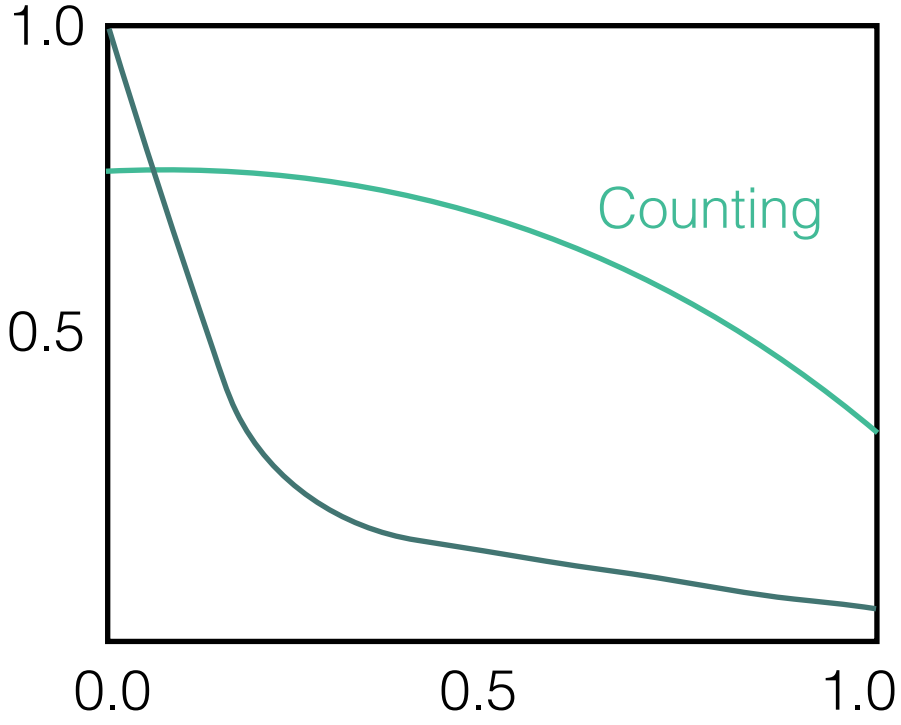

DQE (Detector Quantum Efficiency)
S/N over spatial frequency range

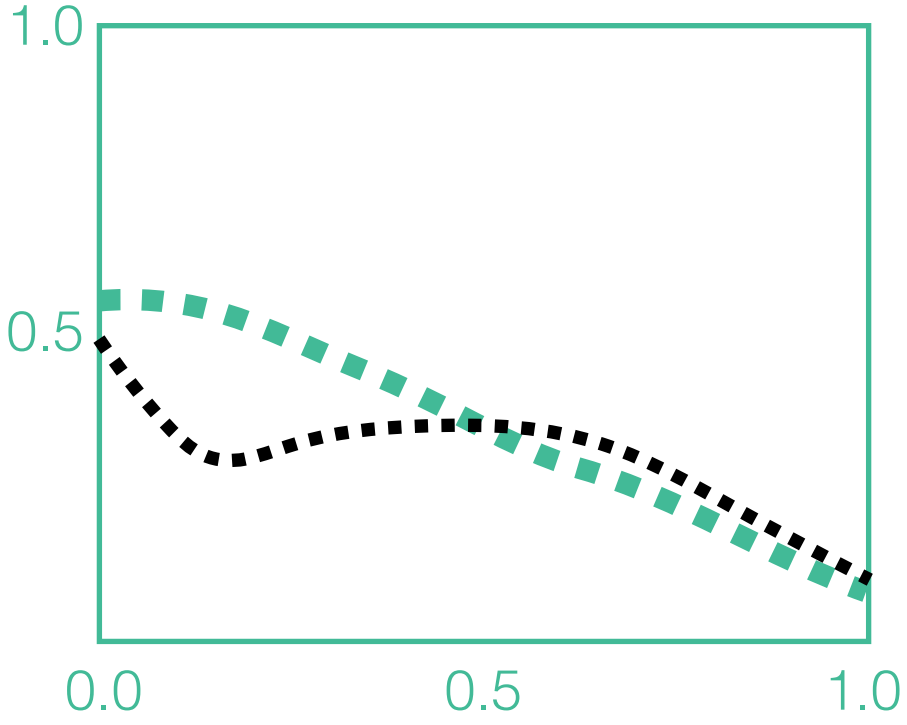

DETECTORS

Detector Performance Characterization

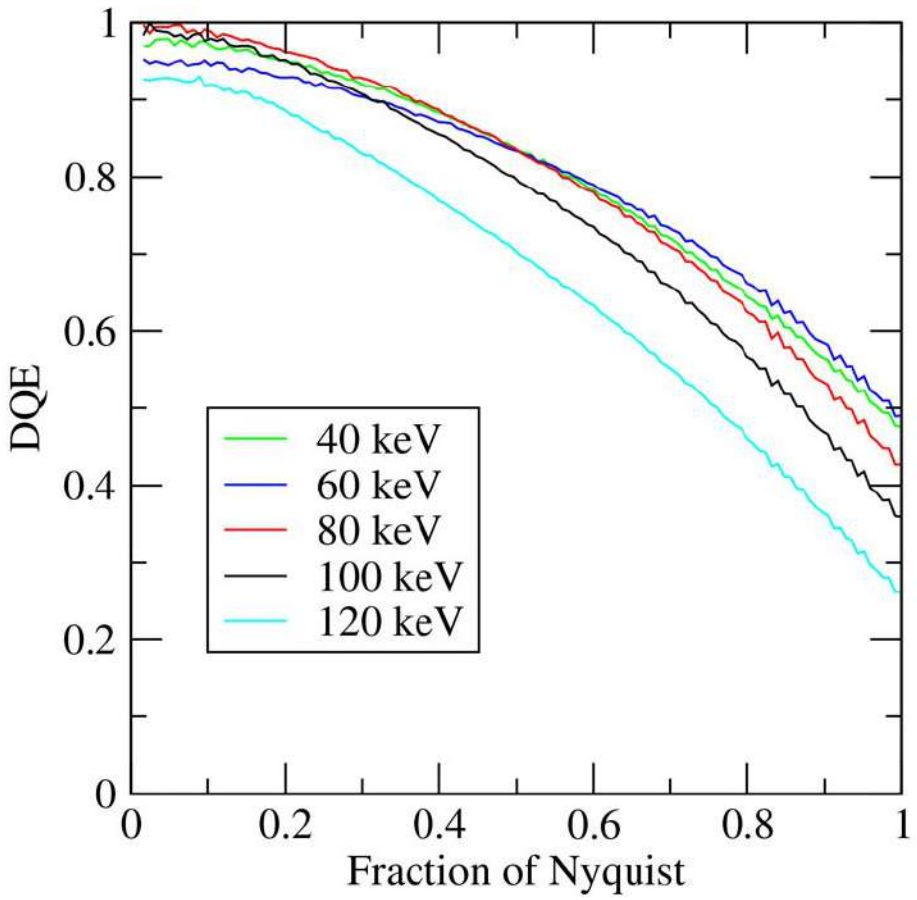

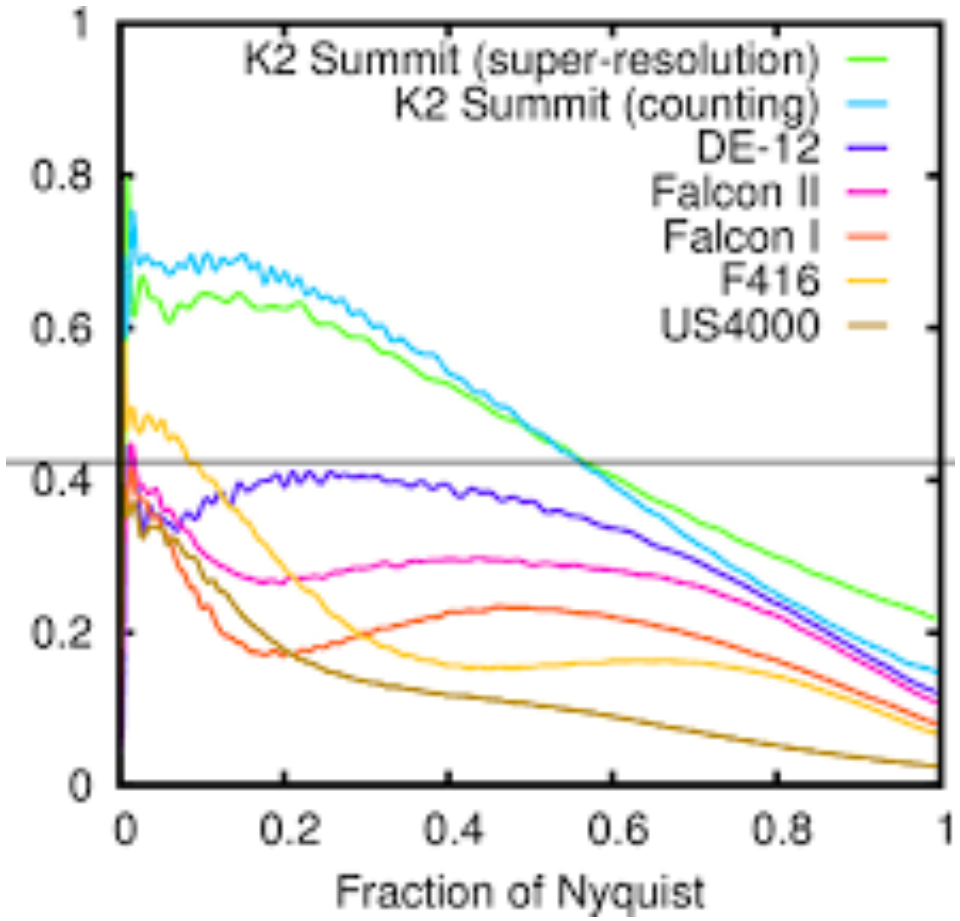

dectris.com

Ruskin, et al JSB

NIH P41 - National Biomedical Technology Research Resources (BTRR)

Krios1

Krios2

Krios3

Krios4

Krios5

Krios6

Krios7

Tecnai F20 Tecnai12

JEOL1230 Helios650

Hitachi 7800

Glacios

Chameleon

ANATOMY OF AN SEM

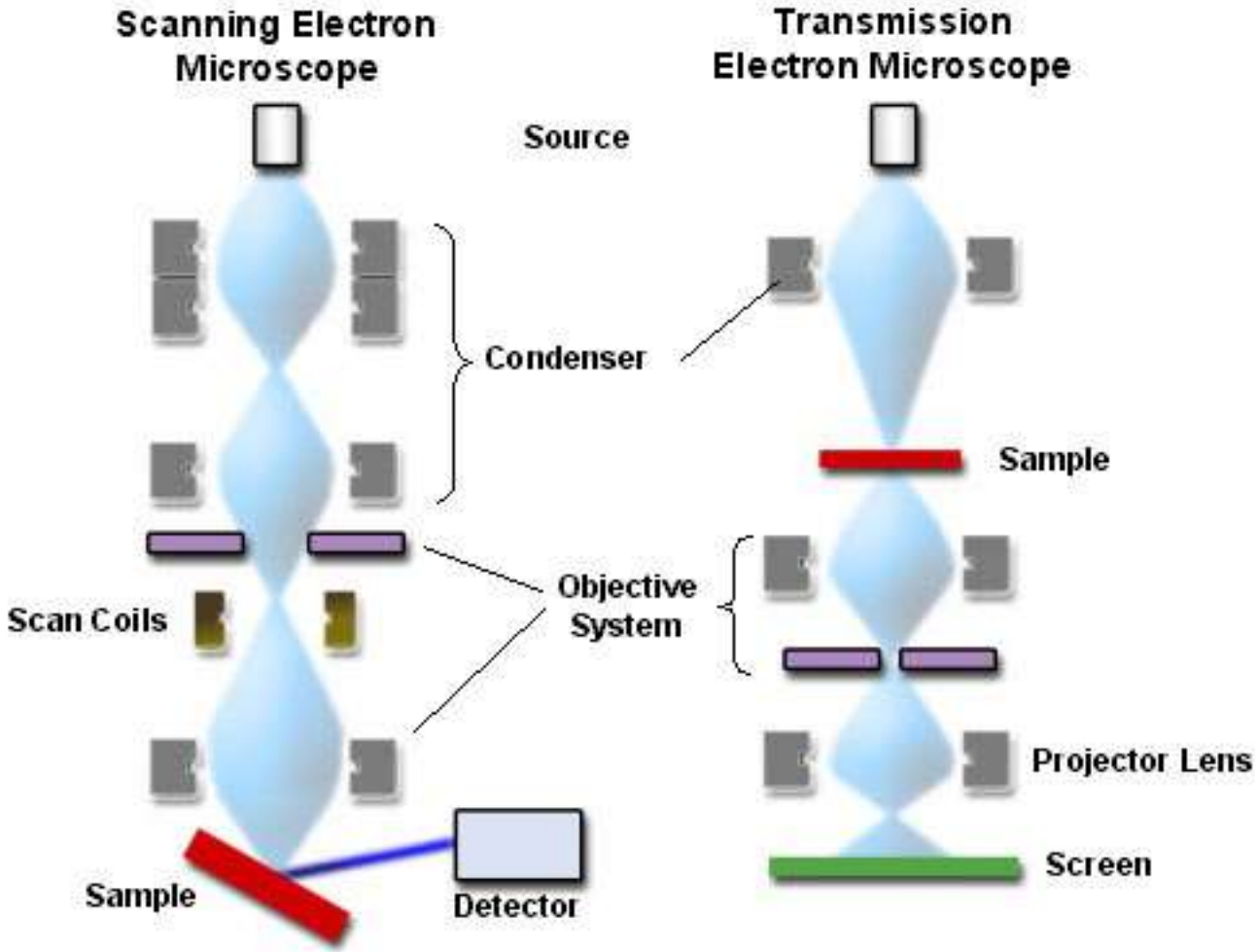

ANATOMY OF AN SEM

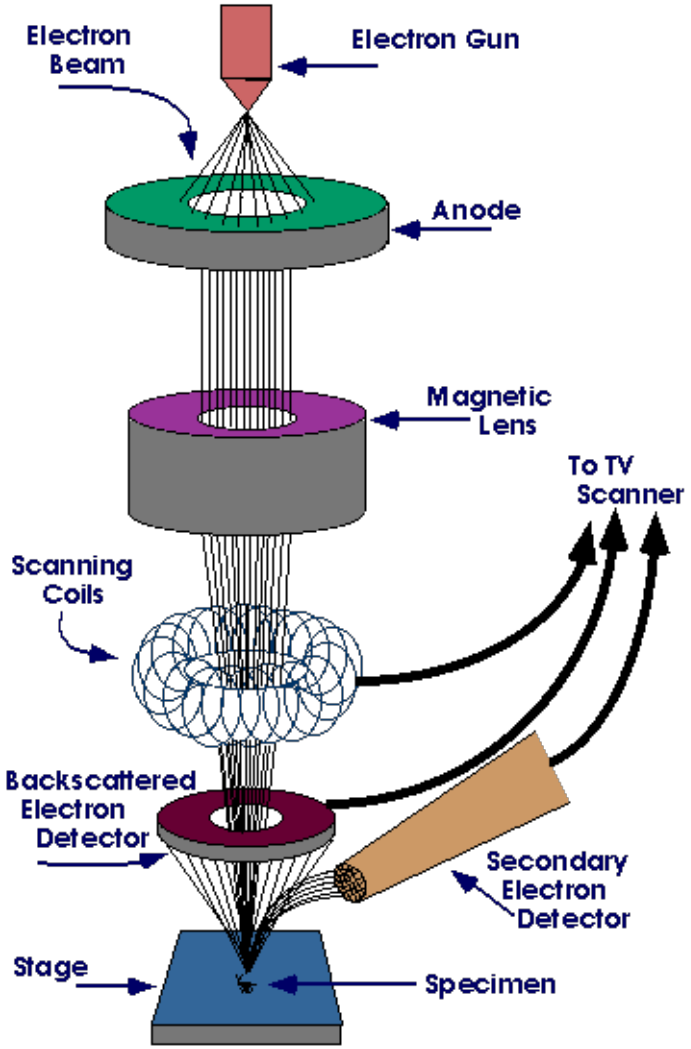

Electron gun: range from tungsten filaments in lower vacuum SEMs to FEGs which need modern high vacuum SEMs

Beam energy: 0.2 – 40 keV is focused by a condenser lens system into a spot of 0.4 – 5 nm

Beam is deflected by very fast scanning coils and rasters the sample surface

Typical resolution of SEM is between 1 and 20 nm where the record is 0.4 nm

ANATOMY OF AN SEM – VACUUM SYSTEMS

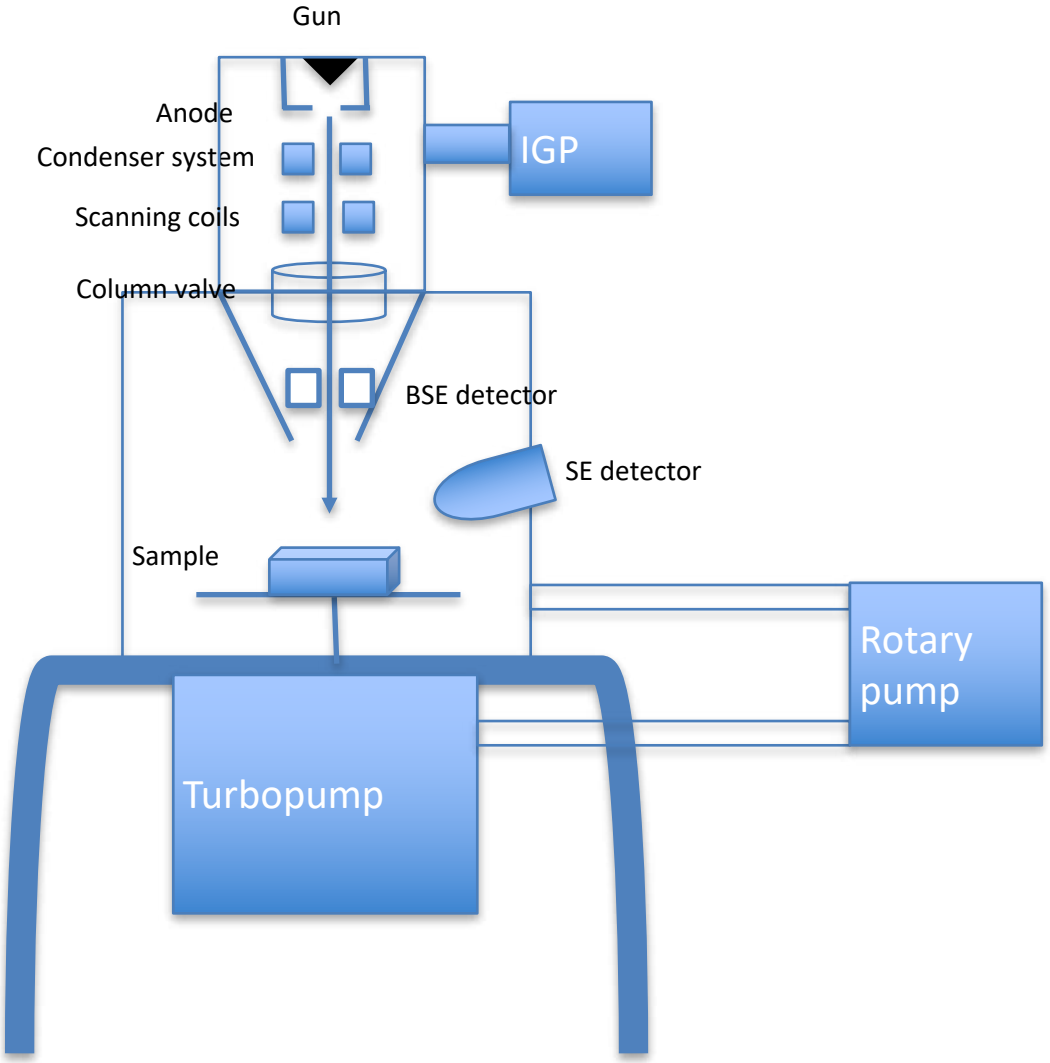

ANATOMY OF AN SEM – BEAM SAMPLE INTERACTIONS

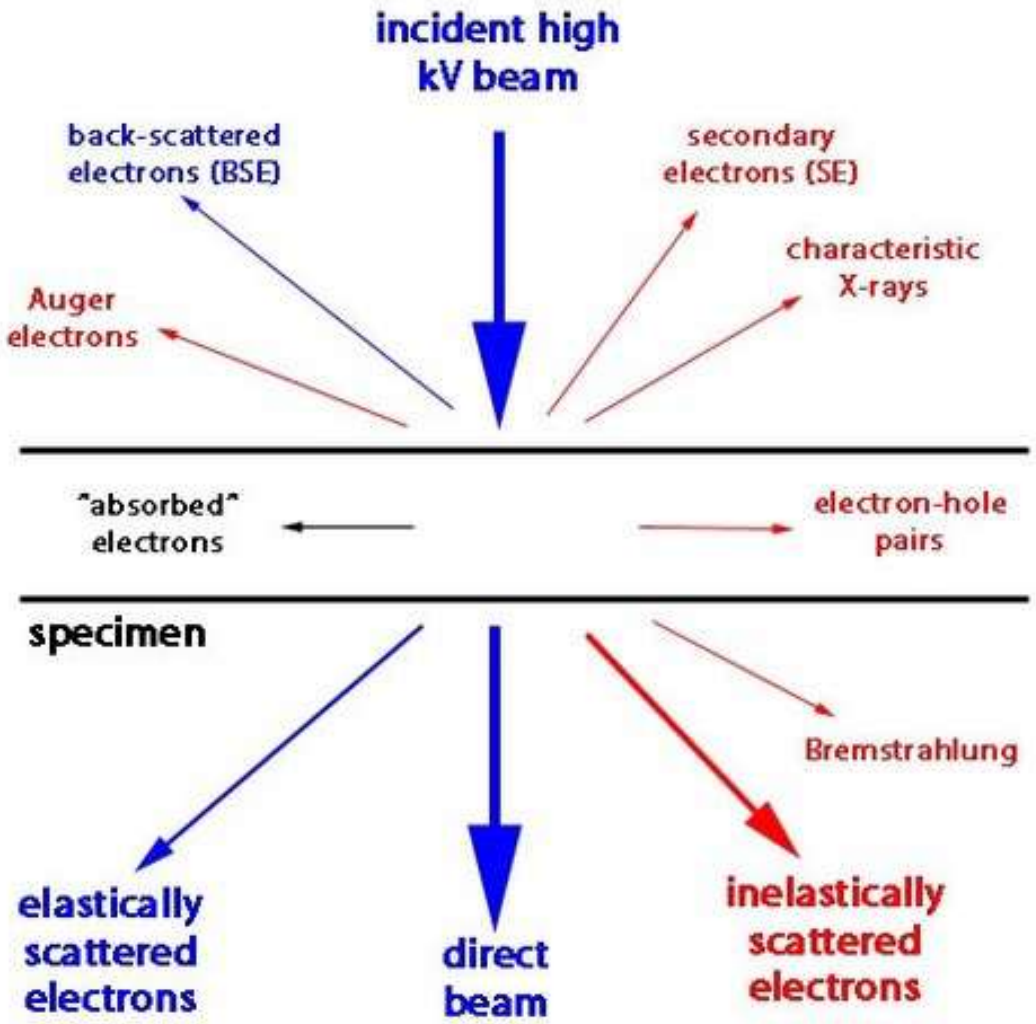

modified from Williams & Carter (1996) Fig. 1.3

ANATOMY OF AN SEM – BEAM SAMPLE INTERACTIONS &IMAGE FORMATION

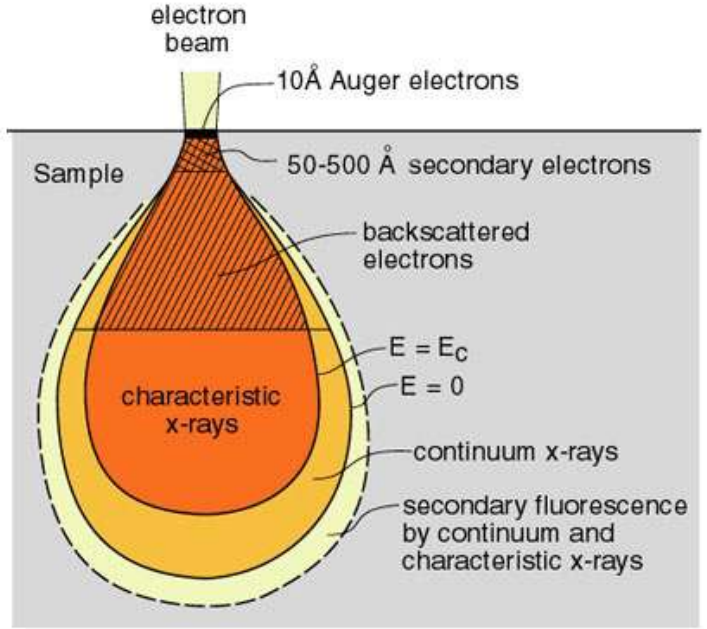

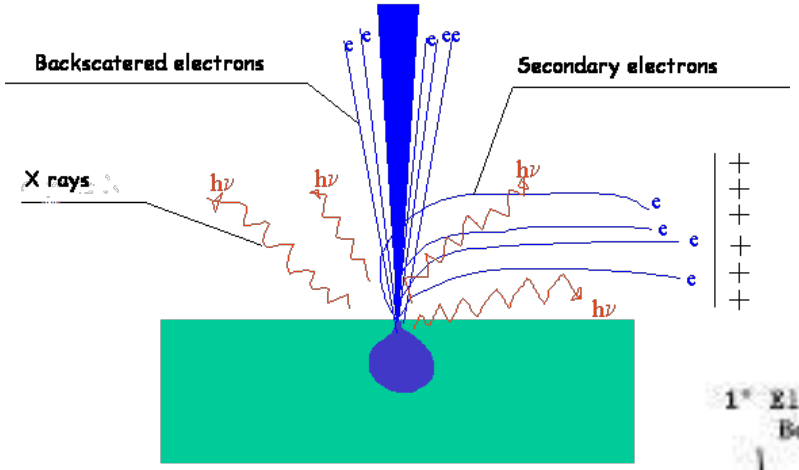

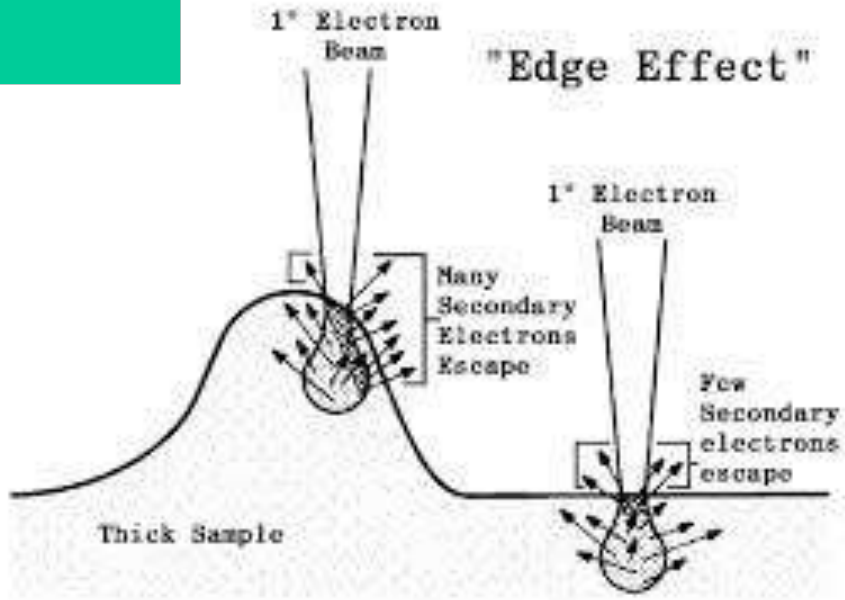

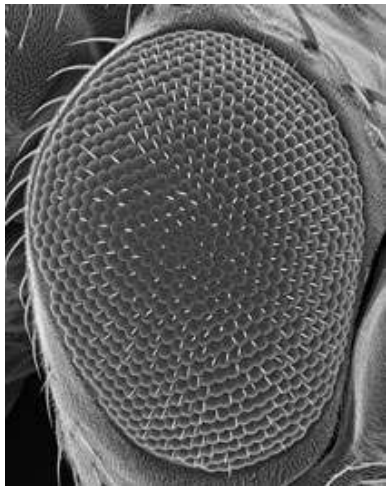

ANATOMY OF AN SEM – BEAM SAMPLE INTERACTIONS &IMAGE FORMATION

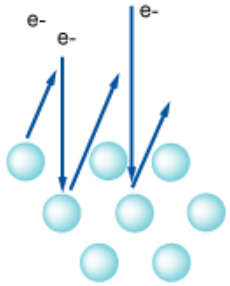

Titanium
atomic number 22

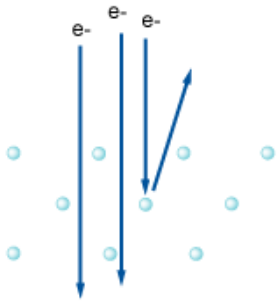

Silicon
atomic number 14

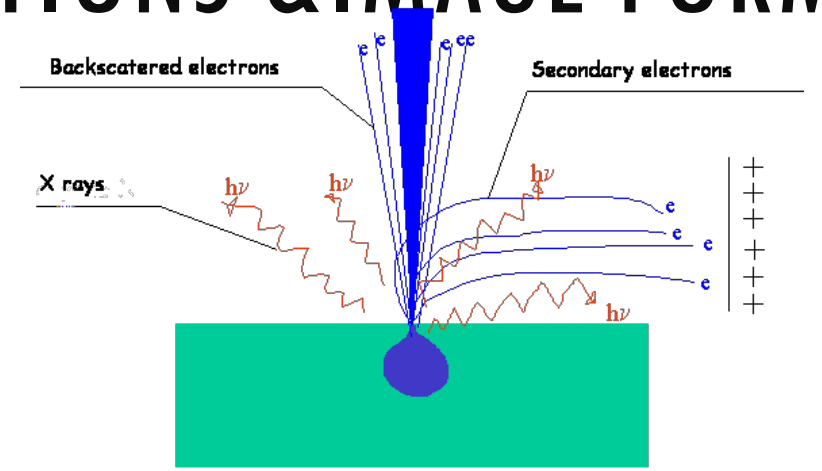

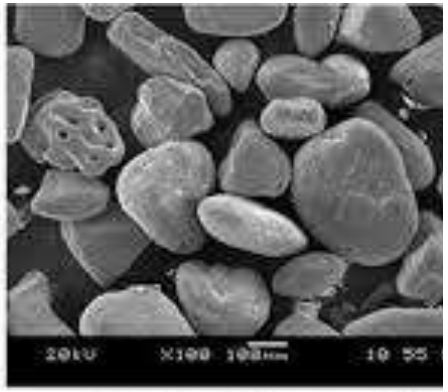

TOOLS OF THE TRADE: MICROSCOPES AND DETECTORS

Questions?

cryoEM 001 : Single Particle Masterclass

1. Building a cryoEM toolkit
2. EM compatible samples
3. EM support films and grids
4. Sample preparation
5. Tools of the trade: microscopes and detectors
6. Microscope operations
7. Data collection strategies
8. Data assessment & QC
9. Data processing:
   - cryoEM IT infrastructure
   - On-the-fly feedback
   - 3D Reconstruction
10. Visualization and validation

ADDITIONAL BACKGROUND READING

Ultramicroscopy 25 (1988) 279–292
North-Holland Amsterdam

CONTRAST TRANSFER FOR FROZEN-HYDRATED SPECIMENS: DETERMINATION FROM PAIRS OF DEFOCUSED IMAGES

Chikashi TOYOSHIMA *
Department of Cell Biology, Stanford University School of Medicine, Stanford, California 94305, USA

and

Nigel UNWIN
Medical Research Council Laboratory of Molecular Biology, Hills Road, Cambridge CB2 2QH, UK

Received 15 January 1987; received in revised form 30 March 1988

Electron imaging of frozen-hydrated biological molecules allows density maps to be obtained directly, without the need for stains or stains. The appearance of such maps may, however, be strongly influenced by the contrast transfer properties, which have not previously been evaluated by quantitative experiments. Here we determine the contribution due to amplitude contrast as a typical (~ 400 Å thick) frozen specimen, consisting of arrays of acetylcholine receptor, by computing pairs of images recorded with different defocus. We find that this specimen is assigned as a "weak-phase-weak-amplitude" object and that the contribution due to amplitude contrast is 7%.

1. Introduction

It is now well established that the linear theory of image formation provides a good approximation in accounting for the contrast present in electron micrographs of thin biological specimens (see ref. [1], for a recent review). In this approximation, the phase contrast produced by defocusing modulates components of the object having different spacings as $\sin \chi(v)$ (χ is the phase shift of the scattered wave and v is the spatial frequency; see section 2) causing them to be recorded with different weights [2]. Thus there is a direct relation between the object and the image, and it is possible to compensate computationally for the variation in $\sin \chi(v)$ (i.e. the phase contrast transfer function) to derive a more accurate representation of the densities composing the specimen [3,4].

Compensation for the effect of the contrast transfer function (CTF) is not usually needed in the analysis of images of negatively stained molecules, where amplitude contrast, which modulates as $\cos \chi(v)$, largely makes up for the reduction in phase contrast that occurs at low resolution [4]. However, with unstained, ice-embedded specimens [5–7] the amplitude contrast, in the absence of heavy metal salts, has a weaker effect and compensation is more likely to be necessary [8]. In addition, specimens preserved by freezing may contain more precise information about the structure, making the accuracy of the compensation – and hence the exact proportion of the amplitude contrast – more critical. The corrections are most important with small crystalline arrays and isolated particles, where electron diffraction cannot be used to obtain a measure of the unmodulated strengths of different spatial components [9]; yet quantitative measurements of the influence of amplitude contrast in such cases have not so far been made

* Present address: Medical Research Council Laboratory of Molecular Biology, Hills Road, Cambridge CB2 2QH, UK.

0304-3991/88/$03.50 © Elsevier Science Publishers B.V.
(North-Holland Physics Publishing Division)

Toyoshima & Unwin 1988

ELSEVIER
Ultramicroscopy 81 (2000) 83–98
ultramicroscopy
www.elsevier.nl/locate/ultramic

Correction of high-resolution data for curvature of the Ewald sphere

David J. DeRosier*
W.M. Keck Institute for Cellular Visualization, Rosenstiel Basic Medical Sciences Research Center, Brandeis University, MS029, 415 South Street, Waltham, MA 02454, USA

Received 6 April 1999; received in revised form 25 August 1999

Abstract

At sufficiently high resolution, which depends on the wavelength of the electrons, the thickness of the sample exceeds the depth of field of the microscope. At this resolution, pairs of beams scattered at symmetric angles about the incident beam are no longer related by Friedel's law; that is, the Fourier coefficients that describe their amplitudes and phases are no longer complex conjugates of each other. Under these conditions, the Fourier coefficients extracted from the image are linear combinations of independent (as opposed to Friedel related) Fourier coefficients corresponding to the three-dimensional (3-D) structure. In order to regenerate the 3-D scattering density, the Fourier coefficients corresponding to the structure have to be recovered from the Fourier coefficients of each image. The requirement for different views of the structure in order to collect a full 3-D data set remains. Computer simulations are used to determine at what resolution, voltage and specimen thickness the extracted coefficients differ significantly from the Fourier coefficients needed for the 3-D structure. This paper presents the theory that describes this situation. It reminds us that the problem can be treated by considering the curvature of the Ewald sphere or equivalently by considering that different layers within the structure are imaged with different amounts of defocus. The paper presents several methods to extract the Fourier coefficients needed for a 3-D reconstruction. The simplest of the methods is to take images with different amounts of defocus. For helical structures, however, only one image is needed. © 2000 Elsevier Science B.V. All rights reserved.

Keywords: Electron microscopy; Depth of field

1. Introduction

The assumption in three-dimensional (3-D) image reconstruction is that the image is a projection of the 3-D structure [1]. This assumption breaks down if the object does not obey the weak phase object approximation or if size of the specimen exceeds the depth of field of the microscope. This paper considers the latter problem only. The assumption that the image is a projection breaks down at sufficiently high resolution [2] at which resolution the thickness of the specimen exceeds the depth of field of the microscope.

* Tel.: +1-781-7362494; fax: +1-781-7362419.
E-mail address: derosier@brandeis.edu (D.J. De Rosier)

0304-3991/00/$ - see front matter © 2000 Elsevier Science B.V. All rights reserved.
PII: S0304-3991(99)00120-5

DeRosier 2000

ELSEVIER
Available online at www.sciencedirect.com
science direct
Ultramicroscopy 106 (2006) 376–382
ultramicroscopy
www.elsevier.com/locate/ultramic

Ewald sphere correction for single-particle electron microscopy

Matthias Wolf[a], David J. DeRosier[a], Nikolaus Grigorieff[a,b,*]
[a]*Rosenstiel Basic Medical Sciences Research Center, Brandeis University, 415 South Street, Waltham, MA 02454, USA*
[b]*Howard Hughes Medical Institute, Brandeis University, 415 South Street, Waltham, MA 02454, USA*

Received 19 August 2005; received in revised form 9 November 2005; accepted 11 November 2005

Abstract

Most algorithms for three-dimensional (3D) reconstruction from electron micrographs assume that images correspond to projections of the 3D structure. This approximation limits the attainable resolution of the reconstruction when the dimensions of the structure exceed the depth of field of the microscope. We have developed two methods to calculate a reconstruction that corrects for the depth of field. Either method applied to synthetic data representing a large virus yields a higher resolution reconstruction than a method lacking this correction.

PACS: 87.64.Bx; 87.64.Dz

Keywords: Three-dimensional reconstruction; Resolution; Depth of field; FREALIGN

1. Introduction

The three-dimensional (3D) reconstruction of a biological molecule or complex from images of single, isolated particles is an important step in electron microscopy (EM) of macromolecules. The reconstruction algorithms commonly used assume that the images are projections of the three-dimensional (3D) object. Although this assumption is a valid approximation for many situations, it breaks down when the size of the object and the desired resolution exceed the depth of field of the microscope [1]. The present work describes two methods to accommodate the depth of field in the reconstruction and alignment of single particles without the use of tilt or defocus pairs. We demonstrate the validity of the approach using simulations.

2. Theory

2.1. Ewald construction

A 3D reconstruction algorithm can be understood most easily by considering its action in reciprocal space. The Fourier transform of the data from each image does not correspond to a plane through the origin (central section) but rather to the surface of the Ewald sphere (EWS, [2]) that passes through the origin of the 3D Fourier transform. The construction in Fig. 1 shows that the deviation, Δz, between the sphere and a plane increases with increasing resolution (determined by the length of the vector $\boldsymbol{g}$). The value of the Fourier transform of the object differs between the two points B, where the transform is sampled, and B′, where the data corresponding to a projection lies; the larger the difference, the greater the deviation of the image from a projection. The magnitude of the difference depends on the dimensions of the object and is larger for objects having a longer dimension along the beam direction.

The error made in the reconstruction when using the planar approximation depends, therefore, on the resolution, the size of the object, and the radius of the EWS (the wavelength of the radiation). DeRosier [1] performed an analysis of the expected phase error between B and B′ and showed that a phase error of 66° for the planar approximation of a spherical shell, such as a virus, occurs at a resolution $R = \sqrt{2} \times 0.7/(t\lambda)$ (0.7 is a dimensionless empirical factor for a spherical shell, object diameter t and wavelength λ are given in units of Å) [1]. For example, for a virus of 500 Å diameter and a wavelength of 0.025 Å

*Corresponding author. Tel.: +1 781 736 2444; fax: +1 781 736 2419.
E-mail address: niko@brandeis.edu (N. Grigorieff).

0304-3991/$ - see front matter © 2005 Elsevier B.V. All rights reserved.
doi:10.1016/j.ultramic.2005.11.001

Wolf et al. 2006

Ultramicroscopy 184 (2018) 94–99
Contents lists available at ScienceDirect
Ultramicroscopy
journal homepage: www.elsevier.com/locate/ultramic

Estimating the effect of finite depth of field in single-particle cryo-EM

Kenneth H. Downing, Robert M. Glaeser*
Lawrence Berkeley National Laboratory, University of California, Berkeley CA 94720, USA

ARTICLE INFO
Article history:
Received 13 April 2017
Revised 5 August 2017
Accepted 15 August 2017
Available online 19 August 2017

ABSTRACT
The extent to which the resolution varies within a three-dimensional (3-D) reconstruction, when the diameter of an object is large, is investigated computationally. Numerical simulation is used to model ideal three-dimensional point-spread functions at different radial positions within an object. It is shown that reconstructed density maps are affected less than might have been expected when particles are larger than the depth of field. This favorable outcome is attributed mainly to the fact that a point which lies outside the depth of field relative to the center, for some orientations of the object, will also lie within the depth of field for other orientations. We find, as a result, that the diameter of a particle can be as much as four times the depth of field (as defined by a 90° phase-error criterion) before curvature of the Ewald sphere becomes a limiting factor in determining the resolution that can be achieved.

1. Introduction

High-resolution electron microscopy of unstained biological macromolecules (single-particle cryo-EM for short) has recently made significant advances [14]. Three-dimensional density maps of large macromolecules are now being obtained with a resolution in the range from 3 to 4 Å, and in a few cases the resolution has already exceeded 2.5 Å [3,4,13]. A fundamental approximation used in this method is that the image intensity is linear in the projected Coulomb potential of the specimen – see, for example, Chapter 4 of [7]. Equivalently, when referring to Fourier space rather than real space, the corresponding approximation is that curvature of the Ewald sphere [6] can be neglected.

Validity of the assumed "projection" approximation requires, among other things, that all portions of the specimen are imaged with the same amount of defocus. This only happens, of course, if the size of the object (i.e. its thickness) is much less than the optical depth of field. As a result, the fundamental approximation, i.e. that the image is a projection of the object, is not expected to be useful if the size of the object is similar to, or much greater than, the depth of field.

This issue has been raised in the past, both in the context of very large virus particles [10,17] and in the context of smaller particles that are randomly distributed within a certain range of Z-heights, which is determined by the overall ice thickness [9]. It seemed to be paradoxical, for example, that high-resolution, three-dimensional reconstructions were obtained from images of icosahedral virus particles whose diameters are larger than the corresponding depth of field [8,12,16]. An often-mentioned resolution of this paradox is that a large number of (symmetry-related) subunits are located at the same Z-height as is the middle of the virus particle. At the same time, it is suggested – reasonably so – that estimation of the defocus value for the image of a virus particle is biased towards the middle, i.e. its center of mass. Thus, if the contrast-transfer-function (CTF) correction for the region near to the middle of a large virus particle is done correctly, a significant amount of signal may be produced from the many subunits whose images have been properly corrected. The suggestion is that this signal can overwhelm the (high-resolution) "noise" contributed by other subunits that lie at Z-heights that are outside the depth of field. Because of this argument, it seemed plausible that the depth of field might be a greater limitation for asymmetric particles than it is for icosahedral virus particles. It thus remains inconclusive that no improvement in the quality of density maps was obtained when computational algorithms were used to compensate for violation of the projection approximation for images of large, icosahedral virus particles [11,15].

We now reopen the question by using computational simulations to better understand what limitations to expect when the size of a particle approaches, and even exceeds, the depth of field for a given resolution. The approach that we have taken is to first calculate noise-free, three-dimensional (3-D) reconstructions of "single points" that are located at different distances from the center of an object. The resulting 3-D point-spread functions are then convoluted with high-resolution density maps for atomic models of two peptide structures found in tubulin, the sizes of which are both much smaller than the depth of field for 300 keV

* Corresponding author.
E-mail address: rmglaeser@lbl.gov (R.M. Glaeser).

http://dx.doi.org/10.1016/j.ultramic.2017.08.007
0304-3991/© 2017 Elsevier B.V. All rights reserved.

Downing & Glaeser 2017